Feedback and Control

10

We now turn to the way in which the body regulates such things as temperature, oxygen concentration in the blood, cardiac output, number of red or white blood cells, and blood concentrations of substances like calcium, sodium, potassium and glucose. Each of these is regulated by a *feedback loop*. A feedback loop exists if variable x determines the value of variable y, and variable y in turn determines the value of variable x.

Suppose that x is the deviation of a bullet from its desired path. A bullet has no feedback; after it has left the gun, its deviation from the desired path is determined by the initial aim of the gun, fall due to gravity, drift caused by the wind, and air turbulence. An accuracy of one part in 10^4 (about a tenth of an inch in 50 ft) is quite good. A car, on the other hand, is steered by the driver. If deviation from the center of the lane x becomes appreciable, the driver changes y, the position of the steering wheel. The value of y determines x through the steering mechanism and the tires. It is possible to have a car deviate less than 1 ft from the desired position within a lane after driving 3000 miles, an accuracy of one part in 10^7. This is an example of *negative feedback*. If x gets too large, the factors in the feedback loop tend to reduce it.

Negative-feedback systems can generate oscillations of their variables. We see oscillations in physiological systems on many different time scales, from the rhythmic activity of the heart, to changes in the rate of breathing, to daily variations in body temperature, blood pressure, and hormone levels, to monthly variations such as the menstrual cycle, to annual variations such as hibernation, coloring, fur growth, and reproduction.

It is also possible to have *positive* feedback. Two bickering children can goad each other to new heights of anger. Positive feedback initiates the action potential described in Chap. 6: depolarization of the axon leads to increased sodium permeability, which further speeds depolarization. Blood pressure is regulated in part by sensors in the kidney. A patient with high blood pressure may suffer damage to the blood vessels, including those feeding the kidneys, which reduces the blood pressure at the sensors. The sensors then ask for still higher blood pressure, which accelerates the damage, which leads to still higher blood pressure, and so on.

The simplest feedback loop consists of two processes: one in which y depends on x and another in which x depends on y. The loop can have many more variables. Steering the car, in addition to the variables of lane position and steering-wheel position, involves vision, neuromuscular processes, all of the variables in the automobile's steering mechanism, and the Newtonian mechanics of the car's motion—with external variables such as the behavior of other drivers continually bombarding the system.

Sections 10.1–10.3 deal with the relationships between the feedback variables when the system is in *equilibrium* or in the *steady state,* and none of the variables are changing with time. The techniques for determining the operating point—the steady-state values of the variables—are graphical and can be applied to any system if the relationship among the variables is known.

When the system is not at equilibrium, it returns to the equilibrium point if the system is stable. Although the equations describing this return to equilibrium are usually not linear, Sects. 10.4–10.7 discuss how linear systems behave when they are not at the operating point. A linear system may " decay" exponentially to the steady-state values or it may exhibit oscillations.

Most systems are not linear. Section 10.8 discusses systems described by nonlinear equations in one or two dimensions, introducing some of the vocabulary and graphical techniques of nonlinear systems analysis. It closes with an example of resetting the phase of a biological oscillator. Section 10.9 introduces the ideas of *period doubling* and *chaotic behavior* through difference equations and the *logistic map*. It then describes a *linear map* that appears to be chaotic but is not. Section 10.10 shows how a linear differential equation that depends on a fixed delay in the variable can exhibit

R. K. Hobbie, B. J. Roth, *Intermediate Physics for Medicine and Biology*,
DOI 10.1007/978-3-319-12682-1_10,

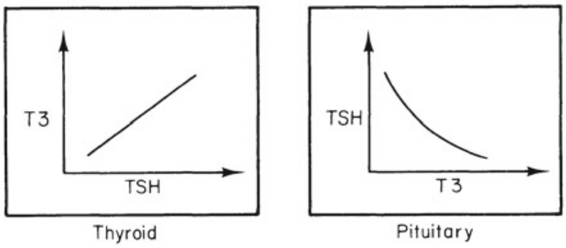

Fig. 10.1 Schematic curves of the relationship between thyroid hormone (*T3*) and thyroid stimulating hormone (*TSH*) in the thyroid gland and in the pituitary

either damped or continuous oscillations. Section 10.11 summarizes the earlier sections, and Sect. 10.12 gives several biological examples.

A great deal of work was done on modeling physiological feedback systems between 1950 and 1975. Books from that era include Riggs (1970) and Stark (1968). More information about mathematical modeling in biology and medicine can be found in Murray (2007, 2008) and Keener and Sneyd (2008a, 2008b).

10.1 Steady-State Relationships Among Variables

Any feedback loop can be broken down, conceptually at least, into separate processes that relate a dependent variable to an independent variable and possibly to some other parameters. Figure 10.1 shows an example. In the first process the thyroid gland, in response to thyroid-stimulating hormone (TSH) from the pituitary, produces the thyroid hormones thyroxine (T4) and tri-iodothyronine (T3). An increase of TSH increases production of T3 and T4. These processes depend on other parameters, such as the amount of iodine available in the body to incorporate into the T3 and T4. In the second process, the pituitary increases the production of TSH if the concentration of T3 in the blood falls. It may also respond to T4 and other variables as well. (This is an oversimplification. The pituitary actually responds to hormones secreted by the hypothalamus. The hypothalamus is responding to the levels of T3 and T4.)

For a quantitative example, consider a simple model relating the amount of carbon dioxide in the alveoli (air sacs of the lung) and the rate of breathing (ventilation rate). If the body is producing CO_2 at a constant rate, a given ventilation rate corresponds to a definite value of P_{CO_2}, the partial pressure of carbon dioxide in the alveoli. In the steady state the amount of CO_2 exhaled (the volume of gas leaving the lungs per minute times P_{CO_2}) is just equal to the amount produced

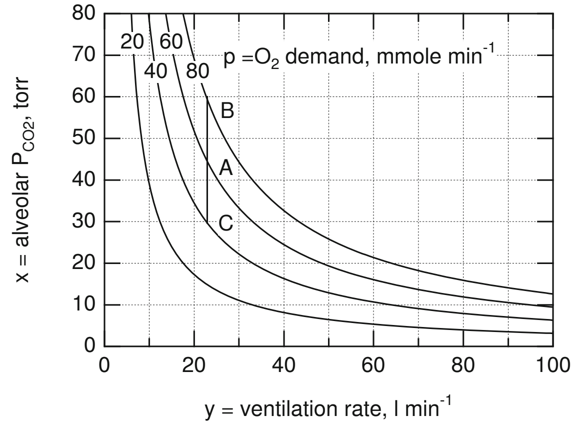

Fig. 10.2 The pressure of CO_2 in the alveoli of the lungs decreases as the ventilation rate is increased. The different curves correspond to different total metabolic rates

in the body. Figure 10.2 shows this relationship when the pH and P_{O_2} of the blood are fixed. As ventilation rate rises, P_{CO_2} falls. We are ignoring several other feedback loops (Riggs 1970, pp. 401–418). If the metabolic rate rises, P_{CO_2} also rises. Experiments show that ventilation rate y and alveolar P_{CO_2} (which we will call x) are related by (Riggs 1970)

$$x = \frac{15.47p}{y - 2.07}. \tag{10.1}$$

In these equations y (the independent variable) is measured in l min^{-1}, x (the dependent variable) is in torr, and parameter p is the body's oxygen consumption in mmol min^{-1}. A typical resting person requires $p = 15$ mmol min^{-1}.

Equation 10.1 can be derived using a simple model for respiration. Let the metabolic rate of the body be described by o, the rate of oxygen consumption in mol s^{-1}. The respiratory quotient F relates o to the rate of CO_2 production, so

$$(\text{rate of } CO_2 \text{ production}) = Fo. \tag{10.2}$$

A typical value of F is 0.8.

Carbon dioxide is removed from the body by breathing. If the rate at which air flows through the alveoli is[1] $(dV/dt)_{\text{alveoli}}$ in m^3 s^{-1}, then the rate of removal is obtained from the ideal-gas law:

$$(\text{rate of CO}_2 \text{ removal}) = \frac{x(dV/dt)_{\text{alveoli}}}{RT}.$$

The rate $(dV/dt)_{\text{alveoli}}$ is less than the ventilation rate y because air in the trachea and bronchi does not exchange

[1] Strictly speaking, $(dV/dt)_{\text{alveoli}}$ is not the derivative of a function V. (It always has a positive value, and the lungs are not expanding without limit!) We use the notation to remind ourselves that it is the rate of air exchange in the alveoli.

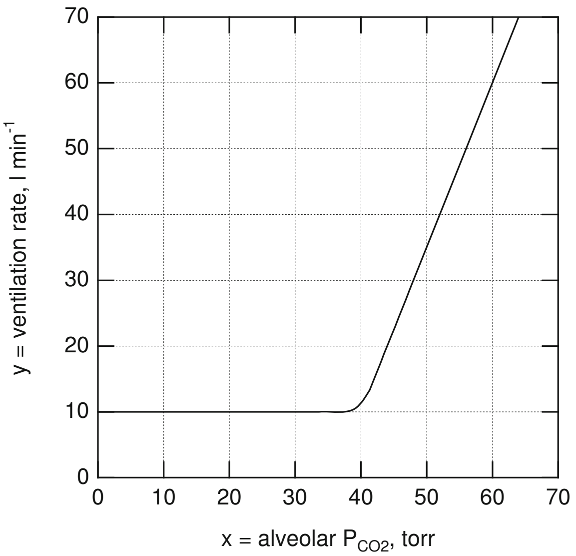

Fig. 10.3 When P_{CO_2} in the blood rises above 40 torr, the breathing rate increases

oxygen or carbon dioxide with the blood: $(dV/dt)_{\text{alveoli}} = y - b$. Therefore

$$\text{(rate of } CO_2 \text{ removal)} = \frac{x(y-b)}{RT}. \qquad (10.3)$$

In equilibrium the rate of production is equal to the rate of removal, so

$$Fo = \frac{x(y-b)}{RT}$$

or

$$x = \frac{RTFo}{y-b}. \qquad (10.4)$$

With the proper conversion of units from p to o, this is Eq. 10.1.

If the metabolic rate were to change without a change in breathing rate, $x = P_{CO_2}$ would change drastically. Suppose that someone exercises moderately so that $p = 60$ mmol min^{-1}, $y = 23$ l min^{-1}, and $x = 44$ torr, point A in Fig. 10.2. If ventilation rate y remained constant while p rose to 80 mmol min^{-1}, $x = P_{CO_2}$ would soar to about 60; if p fell to 40, x would drop to 30. Feedback ensures that this does not happen. One of the feedback mechanisms consists of an area of the brain stem that senses the value of $x = P_{CO_2}$ and causes y to change. Figure 10.3 shows a typical curve for a 70-kg male (Patton 1989, p. 1034). (The concentration of CO_2 in blood is nearly the same as in the alveoli.)

10.2 Determining the Operating Point

We now have two processes relating the steady-state values of x and y. For alveolar gas exchange, we know x as a function of y: $x = g(y, p)$. For the regulatory mechanism, we know $y = f(x)$. Together, these constitute a feedback loop, Fig. 10.4. To find the *operating point*, these two equations must be solved simultaneously. The easiest way to do this is to plot them on the same graph as in Fig. 10.5. When $p = 60$ mmol min^{-1}, the operating point is at A. In a plot like this the horizontal axis represents the independent variable for one process and the dependent variable for the other.

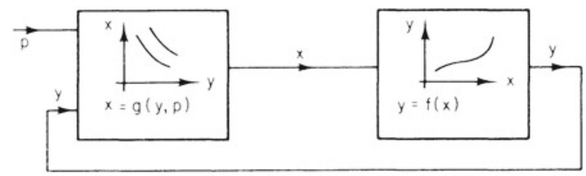

Fig. 10.4 A general feedback loop. Either box may involve some parameters

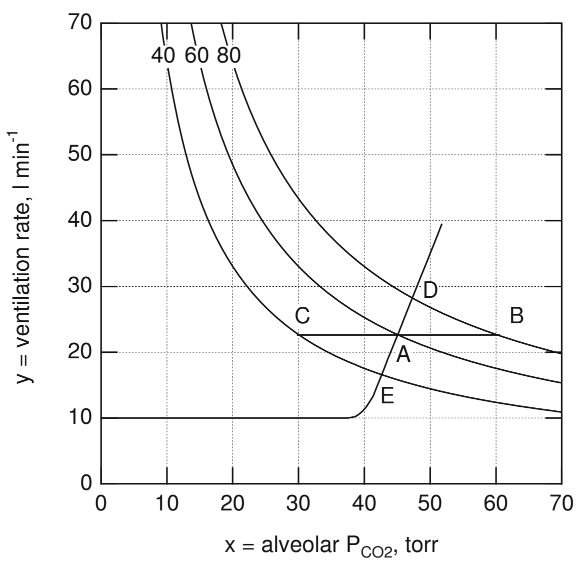

Fig. 10.5 Regulation of the breathing rate. A change of metabolic rate (parameter p) causes a change in ventilation rate y, so that $x = P_{CO_2}$ does not change as much

If the feedback loop includes several variables, for example

$$x = f(w), \quad y = g(x), \quad z = h(y), \quad w = i(z),$$

we can combine three of these equations to get $x = F(y)$ and plot it with $y = g(x)$.

10.3 Regulation of a Variable and Open-Loop Gain

We can also see from Fig. 10.5 how feedback causes y to change in response to a change in parameter p to reduce the change in x. If y does not change, a change of p from 60 to

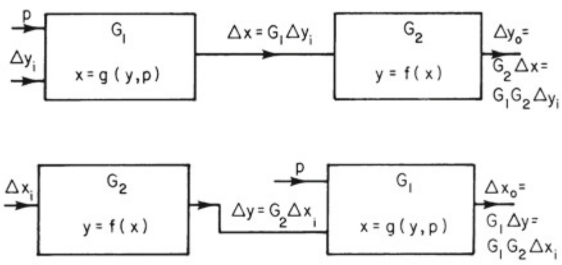

Fig. 10.6 The open loop gain is calculated by opening the loop at any point. **a** Loop opened in y. **b** Loop opened in x

80 causes the operating point to go from A to B. In fact, y increases so that the new operating point is at D. The feedback loop is said to regulate the value of x.

The *gain* of each box in Fig. 10.4 is the ratio of the change in the output variable to the change in the input variable. For the first box

$$G_1 = \left(\frac{\Delta x}{\Delta y}\right)_{\text{box } g,\ p \text{ fixed}} = \left(\frac{\partial x}{\partial y}\right)_{\text{box } g,\ p \text{ fixed}} = \left(\frac{\partial g}{\partial y}\right)_p . \tag{10.5}$$

For the second box,

$$G_2 = \left(\frac{\Delta y}{\Delta x}\right)_{\text{box } f} = \left(\frac{\partial y}{\partial x}\right)_{\text{box } f} = \frac{\partial f}{\partial x}. \tag{10.6}$$

The product $G_1 G_2$ is called the *open-loop gain* (OLG). Its name comes from the fact that if the feedback loop is opened at any point and a small change is made in the input variable at the opening, the change in the output variable is the open-loop gain times the change in the input variable:

$$\text{OLG} = G_1 G_2 = \left(\frac{\partial x}{\partial y}\right)_{\text{box } g} \left(\frac{\partial y}{\partial x}\right)_{\text{box } f} = \frac{\partial g}{\partial y}\frac{\partial f}{\partial x}. \tag{10.7}$$

The open-loop gain can be calculated by taking the derivatives in either order, which corresponds to breaking the loop after either box (Fig. 10.6).

If the relationships between the derivatives have been plotted as in Fig. 10.5, it may be easiest to evaluate the derivatives graphically. In that case, it is easiest to work with $\partial y/\partial x$ for box g. But $\partial y/\partial x = 1/(\partial x/\partial y)$. Therefore,

$$\text{OLG} = G_1 G_2 = \frac{(\partial y/\partial x)_{\text{box } f}}{(\partial y/\partial x)_{\text{box } g}}. \tag{10.8}$$

It is important to calculate the gain in the direction that causality operates. Going around the loop the wrong way gives the reciprocal of the open-loop gain.

We can now calculate how much feedback reduces the change in x, compared to the case in which there is no feedback and the value of y going into box g is held fixed. For box g, where $x = g(y, p)$, we can write for small changes in p and y

$$\begin{aligned}\Delta x &= \left(\frac{\partial x}{\partial p}\right)_{y,\ \text{box } g} \Delta p + \left(\frac{\partial x}{\partial y}\right)_{p,\ \text{box } g} \Delta y \\ &= \left(\frac{\partial x}{\partial p}\right)_{y,\ \text{box } g} \Delta p + G_1 \Delta y.\end{aligned} \tag{10.9}$$

When there is no feedback, Δy is zero and

$$\Delta x = \left(\frac{\partial x}{\partial p}\right)_{y,\ \text{box } g} \Delta p.$$

When there is feedback, there is a value of Δy to be included. If the change in x with feedback is $\Delta x'$, the change in y can be calculated from the second box:

$$\Delta y = \left(\frac{\partial f}{\partial x}\right) \Delta x' = G_2 \Delta x'. \tag{10.10}$$

This can be combined with Eq. 10.9:

$$\Delta x' = \left(\frac{\partial x}{\partial p}\right)_y \Delta p + G_1(G_2 \Delta x') = \Delta x + G_1 G_2 \Delta x'$$

and solved for $\Delta x'$:

$$\Delta x' = \frac{\Delta x}{1 - G_1 G_2} = \frac{\Delta x}{1 - \text{OLG}}. \tag{10.11}$$

The effect of feedback is to cause a change in y that reduces the change in x by the factor $1 - \text{OLG}$. When the feedback is negative, the open-loop gain is negative, $1 - \text{OLG}$ is greater than one, and there is a reduction in Δx. If the feedback is positive and the open-loop gain is less than one, $\Delta x'$ is larger than Δx.

For the respiration example, the equations for each box are

$$\begin{aligned} x &= g(y, p) = \frac{15.47p}{y - 2.07}, \\ y &= f(x) = \begin{cases} 10, & x \le 40, \\ 10 + 2.5(x - 40), & x > 40. \end{cases}\end{aligned} \tag{10.12}$$

The derivatives are

$$\begin{aligned} \left(\frac{\partial g}{\partial p}\right)_y &= \frac{15.47}{y - 2.07}, \\ G_1 = \left(\frac{\partial g}{\partial y}\right)_p &= -\frac{15.47p}{(y - 2.07)^2}, \\ G_2 = \left(\frac{\partial f}{\partial x}\right) &= 2.5. \end{aligned}$$

At operating point A in Fig. 10.5, the values are

$$x = 45.07, \quad p = 60, \quad y = 22.67,$$
$$\left(\frac{\partial g}{\partial p}\right)_y = 0.757, \tag{10.13}$$
$$G_1 = -2.19, \quad G_2 = 2.5, \quad \text{OLG} = -5.48.$$

If p changes from 60 to 62, then without feedback $\Delta x = (0.757)(2) = 1.5$. With feedback, $\Delta x' = 1.5/(1 + 5.48) = 0.23$.

10.4 Approach to Equilibrium without Feedback

The technique described in the preceding section allows us to determine the equilibrium state or operating point of a system if we can measure the functions f and g. It does not tell us how the system behaves when it is not at the equilibrium point, nor does it tell us how the system moves from one point to another when parameter p is changed. To learn that, we need an equation of motion for each process or box in the feedback loop. The equation of motion is usually a differential equation. In real systems the differential equation is often nonlinear and difficult to solve. We first consider models described by linear differential equations, and then we consider some of the behaviors of nonlinear systems.

The response of a system cannot be instantaneous. At equilibrium, the rate of exhaling carbon dioxide is the same as the rate of production throughout the body. If the rate of production rises in a certain muscle group, the extra carbon dioxide enters the blood and is distributed throughout the body, and the carbon dioxide concentrations in the blood and alveoli rise gradually.

To develop a quantitative model, assume that all the carbon dioxide in the body is stored in a single well-stirred compartment of volume V_c. This assumption of uniform concentration is certainly an oversimplification. The total number of moles is n and the concentration is n/V_c. The concentration in the blood is related to the partial pressure in the alveoli by a solubility constant α: $n/V_c = \alpha x$. Therefore $dn/dt = \alpha V_c dx/dt$. Moreover, dn/dt is equal to the rate of production (Eq. 10.2) minus the rate of removal (Eq. 10.3):

$$\frac{dx}{dt} = \frac{Fo}{\alpha V_c} - \frac{x(y-b)}{\alpha V_c RT}.$$

We change the definition of F to take account of the fact that o and p are both the rate of oxygen consumption in slightly different units (o is in mol s^{-1} and p is in mmol min^{-1}):

$$\frac{dx}{dt} = \frac{Fp}{\alpha V_c} - \frac{x(y-b)}{\alpha V_c RT}. \tag{10.14}$$

This differential equation depends on both x and y and in fact is nonlinear since the variables are multiplied together in the last term. At equilibrium $dx/dt = 0$ and Eq. 10.14 gives Eq. 10.4.

If y is constant (a constant breathing rate, which could be accomplished by placing the subject on a respirator), then there is no feedback and Eq. 10.14 is a linear differential equation with constant coefficients:

$$\frac{dx}{dt} + \frac{y_0 - b}{\alpha V_c RT}x = \frac{Fp}{\alpha V_c}.$$

It can be solved using the techniques of Appendix F. Suppose that for $t \le 0$, $p = p_0$, $x = x_0$, and $y = y_0$. For $t > 0$ the subject exercises, so that $p = p_0 + \Delta p$, $x = x_0 + \xi$, and y is unchanged. The equation then becomes

$$\frac{d\xi}{dt} + \frac{y_0 - b}{\alpha V_c RT}\xi = \frac{F\Delta p}{\alpha V_c}. \tag{10.15}$$

The homogeneous equation is

$$\frac{d\xi}{dt} + \frac{1}{\tau_1}\xi = 0, \tag{10.16}$$

where the time constant is

$$\tau_1 = \frac{RT\alpha V_c}{y_0 - b}. \tag{10.17}$$

The homogeneous solution is $\xi = Ae^{-t/\tau_1}$. The particular solution is

$$\xi = \frac{FRT}{y_0 - b}\Delta p = a\,\Delta p,$$

so the complete solution is $\xi = a\,\Delta p + Ae^{-t/\tau_1}$. We now use the initial condition to determine A. At $t = 0$ $\xi = 0$, so $A = -a\,\Delta p$. The complete solution without feedback that matches the initial condition is

$$x - x_0 = a\,\Delta p(1 - e^{-t/\tau_1}). \tag{10.18}$$

Figure 10.7 shows how x changes with time on a plot of x vs. t and a plot of y vs. x. The dots are spaced at equal times.

10.5 Approach to Equilibrium in a Feedback Loop with One Time Constant

Suppose now that y is allowed to change and that $\eta = y - y_0$. We can write the equation for the change in x, Eq. 10.14 as

$$\begin{aligned}\frac{d\xi}{dt} = \frac{dx}{dt} &= \frac{Fp_0}{\alpha V_c} + \frac{F\Delta p}{\alpha V_c} - \frac{(x_0+\xi)(y_0-b+\eta)}{\alpha V_c RT}\\ &= \underbrace{\frac{Fp_0}{\alpha V_c} - \frac{x_0(y_0-b)}{\alpha V_c RT}}_{=0} + \frac{F\Delta p}{\alpha V_c} - \frac{\xi(y_0-b)}{\alpha V_c RT}\\ &\quad - \frac{x_0\eta}{\alpha V_c RT} - \frac{\xi\eta}{\alpha V_c RT}.\end{aligned}$$

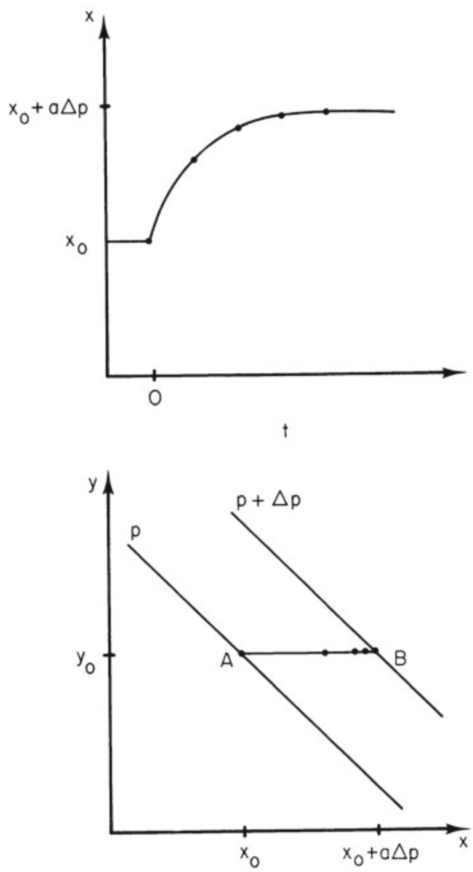

Fig. 10.7 The change in x without feedback in response to a step change in parameter p. **a** Plot of x vs. t. **b** Plot of y vs. x

Multiplying all terms by τ_1 as defined in Eq. 10.17, and identifying

$$G_1 = \left(\frac{\partial g}{\partial y}\right)_p = -\frac{x_0}{y_0 - b},$$

we obtain

$$\tau_1 \frac{d\xi}{dt} = a\,\Delta p - \xi + G_1\eta - \frac{\xi\eta}{y_0 - b}. \qquad (10.19)$$

The product $\xi\eta$ in the last term makes the equation nonlinear. If we assume that the last term can be neglected, we have a linear differential equation

$$\tau_1 \frac{d\xi}{dt} = a\,\Delta p - \xi + G_1\eta. \qquad (10.20)$$

Now assume that the response of the second box is linear and instantaneous, so that

$$\eta = G_2\xi. \qquad (10.21)$$

If this is substituted in the linearized equation, Eq. 10.20, the result is

$$\tau_1 \frac{d\xi}{dt} + (1 - G_1G_2)\xi = a\,\Delta p. \qquad (10.22)$$

The steady-state solution before $t = 0$ is $x_0 = a\,p_0/(1 - G_1G_2)$. At $t = 0$ the oxygen demand is changed to $p_0 + \Delta p$. The new steady-state (inhomogeneous) solution is $\xi = a\,\Delta p/(1 - G_1G_2)$ and the homogeneous solution is $\xi = Ae^{-t/\tau}$ where the time constant is

$$\tau = \frac{\tau_1}{1 - G_1G_2}. \qquad (10.23)$$

(You can show this by dividing each term in Eq. 10.22 by τ_1 and comparing it to the equation for exponential decay.) After combining the homogeneous and inhomogeneous solutions and using the initial condition $\xi(0) = 0$ to determine A, we obtain the final result:

$$\xi = x - x_0 = \frac{a\,\Delta p}{1 - G_1G_2}\left(1 - e^{-t/\tau}\right). \qquad (10.24)$$

This solution has the same form as Eq. 10.18. Both the total change in x and the time constant have been reduced by the factor $1/(1 - G_1G_2)$. The change in y can be determined from $\eta = G_2\xi$. The new solution is plotted along with the old solution in Fig. 10.8. This plot is for a system in which the OLG is $G_1G_2 = -1.3$. The time constant and the change in x are both reduced by $1/2.3$.

It is important to realize that although the feedback reduced the time constant, it has not made x change faster. The curve of $x(t)$ with feedback has always changed less than the curve without feedback, and it has always changed more slowly. The reduction in time constant occurs because x does not change as much with feedback present, so it reaches its asymptotic value more quickly.

This result assumes that box f has a negligible time constant. Applied to the respiratory example, it means that the carbon dioxide-sensing system responds rapidly compared to the time it takes for carbon dioxide levels within the blood to change after a change in p. Figure 10.9a repeats Fig. 10.8 and shows the changes in x and y resulting from a step change in p. When the second time constant is negligible, y is always proportional to x and the system moves back and forth along line AB.

The CO_2 sensors actually take a while to respond. To see what effect this might have, imagine the extreme case where the sensors are very slow compared to the change of carbon dioxide concentration in the blood. In that case, when p changes, y does not change right away. The system behaves at first as if there were no feedback, moving from point A to point C in Fig. 10.9b. As the feedback slowly takes effect, the system moves from C to B. When the exercise ends, the system moves to point D because the subject is breathing too hard. Then it finally moves from D back to A. The actual

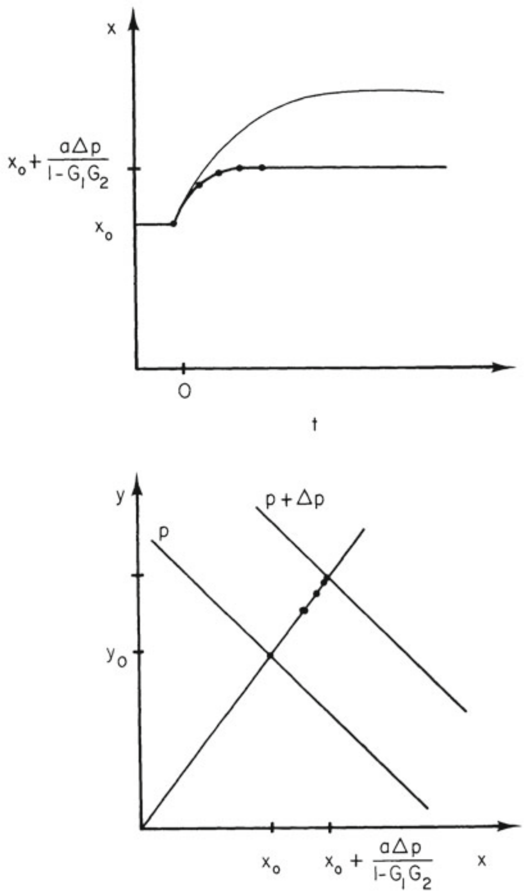

Fig. 10.8 The change in x with feedback in response to a step change in parameter p. **a** Plot of x vs. t. The change in x without feedback is shown for comparison. **b** Plot of y vs. x

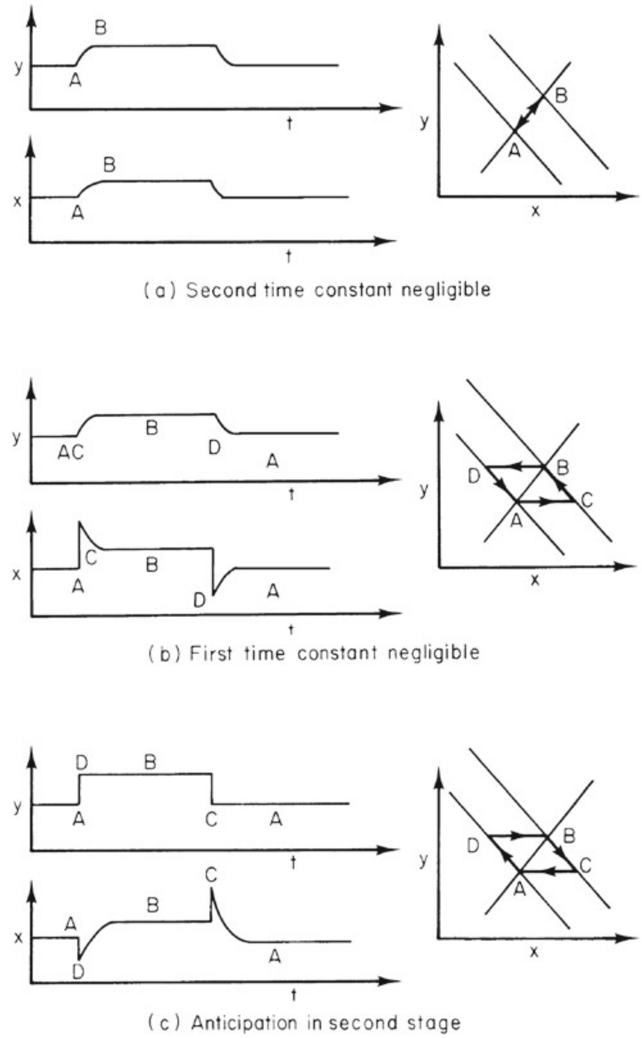

Fig. 10.9 Changes in x and y after a step change in parameter p. **a** The second time constant is negligible compared to the first; x and y move exponentially to their new equilibrium values. **b** The first time constant is negligible; the slow change in y means that there is no feedback at first. **c** The second stage anticipates the change in y that will be required; there is too much feedback at first

system behaves in a manner somewhere between these two extremes, as we will see in the next section.

Consider a third possibility, that a regulatory mechanism anticipates the increased metabolic demand. This might happen if we took deep breaths before we began to exercise, or if additional muscle movement signaled the respiratory control center before the carbon dioxide concentration had a chance to change. Suppose that such anticipation is the only feedback mechanism. With the initiation of exercise, y changes to its final value. The level of carbon dioxide has not yet built up, so the increased ventilation reduces x below its normal value. We can approximate this by point D in Fig. 10.9c. As the increased activity drives x up, the system moves at constant y to point B. When the exercise stops, y drops immediately to the resting value, though carbon dioxide is still coming out of the muscles. The result is that x rises to point C before finally falling back to point A.

Figure 10.10 shows what actually happens in the control of respiration. There is a fast neurological control and a slower chemical control. The result is a combination of the processes in Figs. 10.9a–10.9c.

If we had not made the linear approximation we would not have been able to solve the equation, but the behavior would have been very similar. The nonlinear equation is obtained by substituting the equation for the second box, Eq. 10.21, in Eq. 10.19 instead of Eq. 10.20. The resulting equation is

$$\tau_1 \frac{d\xi}{dt} = a\,\Delta p - (1 - G_1G_2)\xi - \frac{G_2\xi^2}{y_0 - b}. \qquad (10.25)$$

Both this and the linear version are plotted in Fig. 10.11 for $a\,\Delta p = 0$. In each case $d\xi/dt$ is positive when $\xi < 0$ and negative when $\xi > 0$, so ξ approaches zero as time goes on.

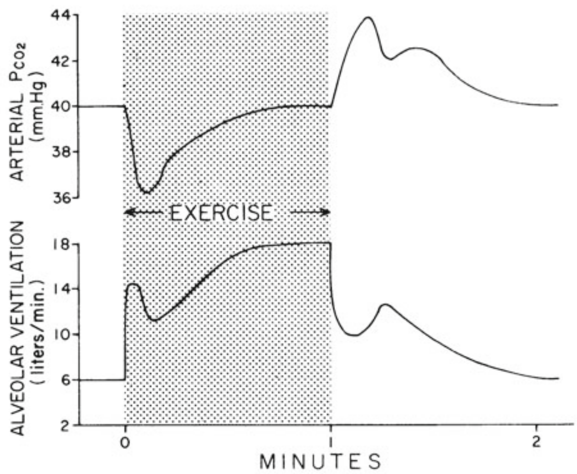

Fig. 10.10 Change of arterial P_{CO_2} and alveolar ventilation in response to exercise. Note that $x = P_{CO_2}$ is in the upper graph and the ventilation rate y is in the lower graph, the opposite of Fig. 10.9. (Reprinted from Guyton (1995) with the permission of Elsevier. Data are extrapolated to humans from dogs. The dog experiments are described in C. R. Bainton (1972). J Appl Physiol 33: 778–787)

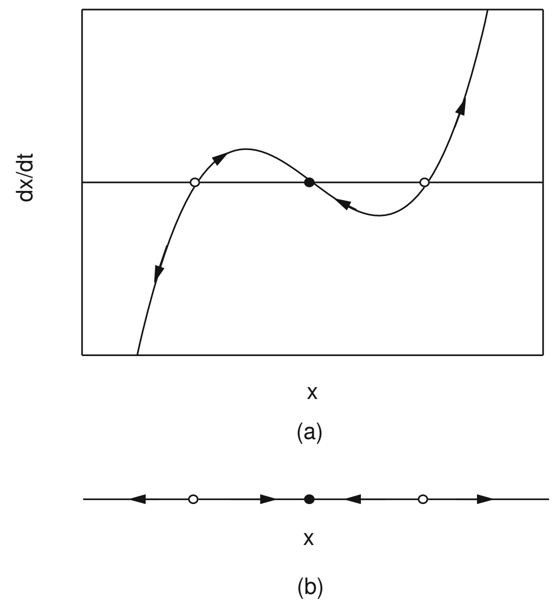

Fig. 10.12 Graphical analysis of the solution to a more complicated differential equation $dx/dt = f(x)$. **a** Plot of dx/dt vs. x. The arrows show the direction that x changes. The open circles show unstable fixed points, and the filled circle is a stable fixed point. **b** The fixed points and the direction of flow are shown on the x axis

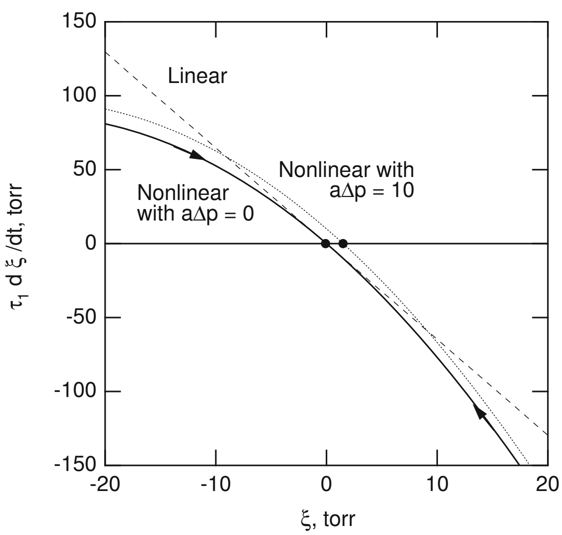

Fig. 10.11 Plots of $\tau_1(d\xi/dt)$ vs. ξ. The straight dashed line is the linear approximation, Eq. 10.22. The parabolas are plots of the nonlinear equation, Eq. 10.25, for two different values of parameter $a\Delta p$. The closed circles show stable fixed points

The direction of evolution of ξ is shown by the arrows on the nonlinear curve. This is often called a *one-dimensional flow*. The variable ξ "flows" to the origin, which is called a *stable fixed point* of the flow. If we change $a\,\Delta p$ to 10, the curve shifts as indicated by the dotted line, and the fixed point moves to a slightly different value of ξ.

This is a particular case of a differential equation in one dependent variable of the form $dx/dt = f(x)$. A great deal about the solution to the general equation can be learned by graphing it as we have done above. When the derivative is positive the function increases with time, and when it is negative it decreases. Figure 10.12a shows a more complicated function, with arrows showing the direction of the flow. The stable fixed point is indicated by a solid circle. There are two *unstable fixed points*, indicated by open circles. If x has precisely the value of an unstable fixed point, it remains there because $dx/dt = 0$. However, if it is displaced even a small amount, it flows away from the unstable point. Figure 10.12b shows just the x axis with the fixed points and the arrows. Stable fixed points are often called *attractors* or *sinks*. The unstable fixed points are called *repellers* or *sources*. Chapter 2 of Strogatz (1994) has an excellent and detailed discussion of one-dimensional flows.

10.6 A Feedback Loop with Two Time Constants

In the preceding section we considered a feedback loop in which only one process had a significant time constant. The other process responded "instantaneously;" its time constant was much shorter. Here we consider the case in which both processes have comparable time constants. We will see that it is possible for such a (linear) system to exhibit damped sinusoidal behavior in response to an abrupt change in one of the parameters. Whether it does or not depends on the relative values of the two time constants and the open-loop gain. We consider both graphical and analytical techniques for solving this problem.

In earlier sections we discussed control of breathing. Equation 10.20 was the linear model for the departure of one variable from equilibrium:

$$\tau_1 \frac{d\xi}{dt} = -\xi + G_1\eta + a\,\Delta p.$$

For the second process, instead of $\eta = G_2\xi$ we assume that the behavior is given by an analogous equation

$$\tau_2 \frac{d\eta}{dt} = -\eta + G_2\xi. \tag{10.26}$$

For negative feedback either G_1 or G_2 must be negative.

We have a special case of a pair of first-order differential equations

$$\begin{aligned} \frac{dx_1}{dt} &= f_1(x_1, x_2), \\ \frac{dx_2}{dt} &= f_2(x_1, x_2). \end{aligned} \tag{10.27}$$

(Here x_1 and x_2 are general variables and have no relationship with the breathing problem considered earlier.)

We first combine the two first-order equations to make a second-order equation which, because we are using linear equations, can be solved exactly. To do this, differentiate Eq. 10.20:

$$\tau_1 \frac{d^2\xi}{dt^2} + \frac{d\xi}{dt} = a\frac{dp}{dt} + G_1\frac{d\eta}{dt}.$$

Substitute Eq. 10.26 in this and obtain

$$\tau_1 \frac{d^2\xi}{dt^2} + \frac{d\xi}{dt} = -\frac{G_1}{\tau_2}\eta + \frac{G_1G_2}{\tau_2}\xi + a\frac{dp}{dt}.$$

To eliminate η, solve Eq. 10.20 for $G_1\eta$ and substitute it in this equation:

$$\tau_1 \frac{d^2\xi}{dt^2} + \frac{d\xi}{dt} = -\frac{\tau_1}{\tau_2}\frac{d\xi}{dt} - \frac{1}{\tau_2}\xi + \frac{a}{\tau_2}p + \frac{G_1G_2}{\tau_2}\xi + a\frac{dp}{dt}.$$

After like terms are combined, the result is

$$\frac{d^2\xi}{dt^2} + \left(\frac{1}{\tau_1} + \frac{1}{\tau_2}\right)\frac{d\xi}{dt} + \frac{1 - G_1G_2}{\tau_1\tau_2}\xi = \frac{a}{\tau_1\tau_2}p(t) + \frac{a}{\tau_1}\frac{dp}{dt}. \tag{10.28}$$

This is another linear differential equation with constant coefficients. The right-hand side is a known function of time, since $p(t)$ is known. The homogeneous equation is very common in physics and is called the *harmonic oscillator equation*. It is usually written in the form

$$\frac{d^2\xi}{dt^2} + 2\alpha\frac{d\xi}{dt} + \omega_0^2\xi = 0, \tag{10.29a}$$

with the identifications

$$2\alpha = \frac{1}{\tau_1} + \frac{1}{\tau_2} = \frac{\tau_1 + \tau_2}{\tau_1\tau_2} \tag{10.29b}$$

and

$$\omega_0^2 = \frac{1 - G_1G_2}{\tau_1\tau_2}. \tag{10.29c}$$

Appendix F shows that as long as $\alpha \geq \omega_0$, the system is critically damped or overdamped and there will be no oscillation or *ringing*. This will be the case if

$$\frac{(\tau_1 + \tau_2)^2}{4\tau_1^2\tau_2^2} \geq \frac{1 - G_1G_2}{\tau_1\tau_2}$$

or

$$\frac{(\tau_1 + \tau_2)^2}{4\tau_1\tau_2} \geq 1 - G_1G_2. \tag{10.30}$$

This equation is symmetric in τ_1 and τ_2. The important parameter is $r = \tau_1/\tau_2$. There is no ringing when

$$\frac{(1 + r)^2}{4r} \geq 1 - G_1G_2.$$

Since the feedback is negative, $G_1G_2 = -|G_1G_2|$. Then there is no ringing if

$$|G_1G_2| < \frac{r}{4} + \frac{1}{4r} - \frac{1}{2}, \quad G_1G_2 < 0. \tag{10.31}$$

If the two time constants are equal ($r = 1$), the right-hand side of Eq. 10.31 is zero. There will be ringing if the open-loop gain has a magnitude greater than zero. For large values of r (say $r > 10$), the equation is approximately $|G_1G_2| < r/4$. If the magnitude of the open-loop gain is larger than this, there will be ringing.

We can see the general behavior of Eqs. 10.20 and 10.26 by examining the behavior of the derivatives. Both derivatives are zero and there is a fixed point when

$$\xi = \frac{a\,\Delta p}{1 - G_1G_2}, \quad \eta = \frac{G_2 a\,\Delta p}{1 - G_1G_2}.$$

For $\Delta p = 0$ the fixed point is at the origin. Figures 10.13 and 10.14 show plots of ξ and η for different values of the gain and damping. The plots of η vs. ξ are called *state-space* plots or *phase-space* or *phase-plane* plots. The plots shown here are spiral to the fixed point. Depending on the values of the gains and time constants (try positive feedback) there can also be exponentially growing solutions. An extensive literature exists analyzing stability for both Eqs. 10.27 and their linearized versions. See Chaps. 5 and 6 of Strogatz (1994) or Chap. 3 of Hilborn (2000). For a visual but nonmathematical analysis, see Abraham and Shaw (1992).

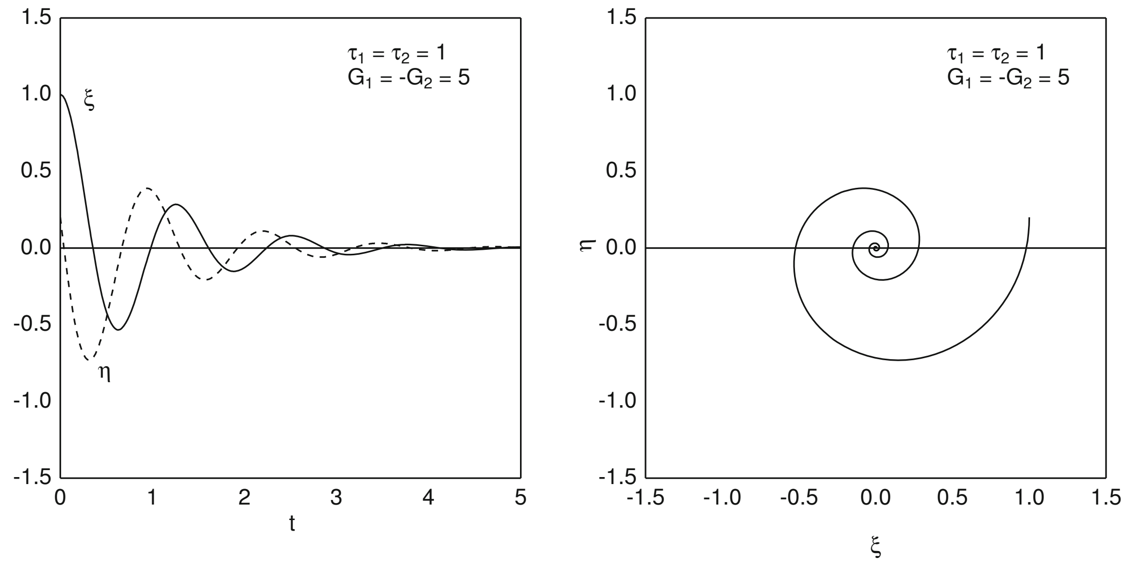

Fig. 10.13 A solution to Eq. 10.28 is plotted that has a value 1 and time derivative 0 when $t = 0$. The variable η is obtained from ξ by using Eq. 10.26. Plots of ξ and η vs. t are shown on the left. A state-space plot of η vs ξ is shown on the right

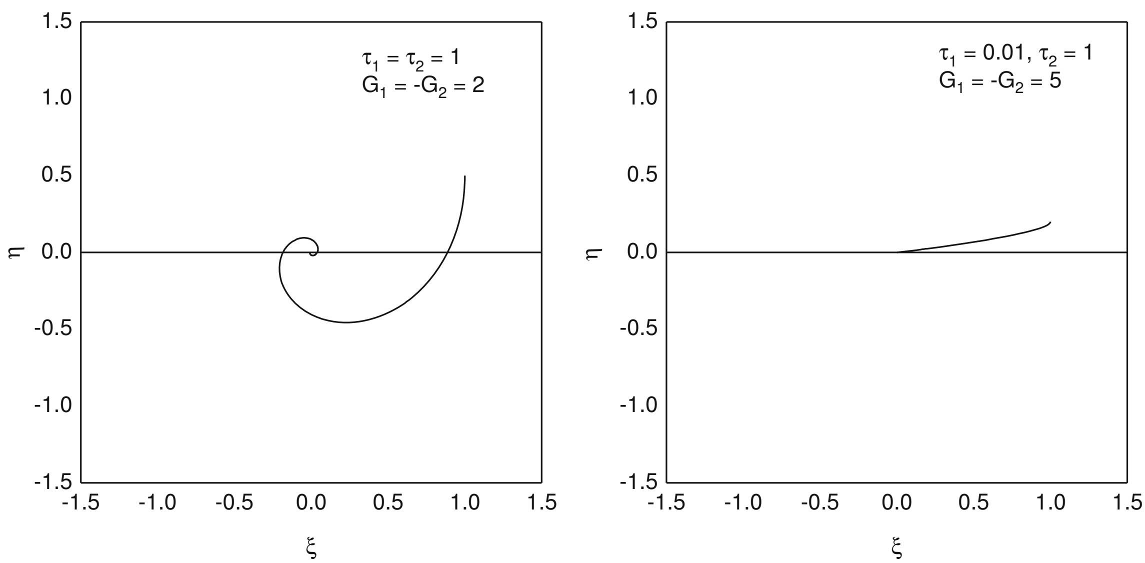

Fig. 10.14 Additional state-space plots for the same initial conditions as in Fig. 10.13, but with different values of the parameters

10.7 Proportional, Derivative, and Integral Control

We have been looking at a particular example of a *control system*. In Sect. 10.4 and 10.5 we considered a system for which, for $t \le 0$, $p = p_0$, $x = x_0$, and $y = y_0$. For $t > 0$ the subject exercised, so that $p = p_0 + \Delta p$, $x = x_0 + \xi$, and $y = y_0 + \eta$. There were two equations of motion, Eqs. 10.20 and 10.21:

$$\tau_1 \left(\frac{d\xi}{dt} \right) + \xi = a\Delta p + G_1 \eta. \tag{10.32}$$

$$\eta = G_2 \xi. \tag{10.33}$$

Combining these we find the steady state solution is

$$\xi = \frac{a\Delta p}{1 - G_1 G_2}. \tag{10.34}$$

The goal of a control system is to make $\xi = x - x_0$ as small as possible as p is varied. In the language of control theory x_0 is called the *set point* or *reference quantity*, x is called the *present value* or *actual output*, and $e = x_0 - x = -\xi$ is called the *controller error*.

At $t = 0$ there is a step change Δp. Without feedback (G_1 or $G_2 = 0$), this causes a change in the steady-state

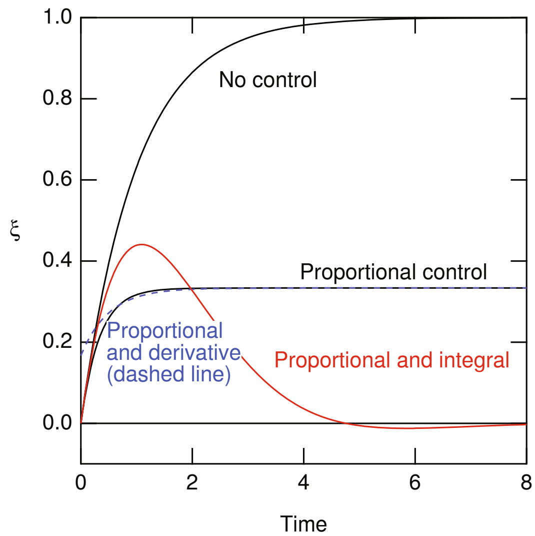

Fig. 10.15 Examples of the different kinds of control: none, proportional, proportional with derivative, and proportional with integral. Derivative reaches the steady-state value more quickly. Integral control allows the error, ξ, to become zero

value $\xi = a\Delta p$. Feedback reduces this to $\xi = a\Delta p/(1 - G_1G_2)$. This is called *proportional control*. The input to the controller (the second box in Fig. 10.4) is ξ.

In *derivative control* an additional signal is introduced on the right hand side of Eq. 10.33, which is proportional to the derivative of the error signal. Usually a combination of proportional and derivative control is used:

$$\eta = G_2\xi + G_2\tau_d\frac{d\xi}{dt}.$$

Factor τ_d has the dimensions of time and gives the relative strength of the derivative control term. Combining this with Eq. 10.32 gives us

$$\tau_1\left(\frac{d\xi}{dt}\right) + \xi = a\Delta p + G_1G_2\xi + \tau_d G_1G_2\left(\frac{d\xi}{dt}\right).$$

Regrouping gives

$$\frac{d\xi}{dt} + \frac{(1 - G_1G_2)}{(\tau_1 - \tau_d G_1G_2)}\xi = \frac{a\Delta p}{(\tau_1 - \tau_d G_1G_2)}.$$

In *integral control* a term

$$\frac{G_2}{\tau_i}\int_0^t \xi(t)dt$$

is added to Eq. 10.33. For a combination of proportional and integral control we have

$$\tau_1\left(\frac{d\xi}{dt}\right) + \xi = a\Delta p + G_1G_2\xi + G_1G_2\frac{1}{\tau_i}\int_0^t \xi(t)dt.$$

This can be rearranged as

$$\tau_1\left(\frac{d\xi}{dt}\right) + (1 - G_1G_2)\xi + \frac{G_1G_2}{\tau_i}\int_0^t \xi(t)dt = a\Delta p.$$

Differentiating gives us the harmonic oscillator equation:

$$\frac{d^2\xi}{dt^2} + \frac{(1 - G_1G_2)}{\tau_1}\frac{d\xi}{dt} + \frac{G_1G_2}{\tau_1\tau_i}\xi = 0.$$

Proportional, proportional plus derivative, and proportional plus integral control are compared in Fig. 10.15. Derivative control causes the abrupt jump in ξ at $t = 0$. However, the offset or steady-state value remains the same as in proportional control. Integral control can reduce the offset to zero, but oscillations are likely. El-Samad et al. (2002) and Khammash and El-Samad (2004) describe proportional and integral control of calcium regulation in cows that have just given birth. LeDuc et al. (2011) review control techniques and how they can be used to manipulate cells in the laboratory.

10.8 Models Using Nonlinear Differential Equations

We have used many models in this book. In Chap. 2 we introduced a linear differential equation that leads to exponential growth or decay, and we used it to model tumor and bacterial growth and the movement of drugs through the body. We briefly examined some nonlinear extensions of this model. In Chap. 4 we modeled diffusion processes with linear equations—Fick's first and second laws—and we used a linear model to describe solvent drag. In Chap. 5 we used the model of a right-cylindrical pore. In Chap. 6 we used both a linear model—electrotonus—and a nonlinear model—the Hodgkin–Huxley equations. In this chapter we introduced a linear model for feedback, and we saw how two linear processes in a feedback loop could lead to oscillations, the linear harmonic oscillator.

Linear models have one advantage: they can be solved exactly. But most processes in nature are not linear. Jules Henri Poincaré realized around 1900 that systems described exactly by the completely deterministic equations of Newton's laws could exhibit wild behavior. Poincaré was studying the three-body problem in astronomy (such as Sun–Earth–Moon). While we are all familiar with the fact that the motion of the Sun–Earth–Moon system is evolving smoothly with time and that eclipses can be predicted centuries in advance, this smooth behavior does not happen for all systems. For certain ranges of parameters (such as the masses of the objects and initial positions and velocities) the solutions can exhibit behavior that is now termed *chaotic*. If we consider the motion that results from two sets of initial conditions that differ from each other only by an infinitesimal amount in one of the variables, we find that in chaotic behavior there can be solutions that diverge exponentially from each other as time goes on, even though the solutions remain bounded. Poincaré developed some geometrical techniques for studying the behavior of such systems. Thorough study of nonlinear systems requires the use of a digital computer. As a result, it has only been since the 1970s that we have realized how often chaotic behavior can occur in a system governed by deterministic equations. With computers we have gained more insight into the properties of chaotic behavior.

Just as the harmonic oscillator provides a model for behavior seen in many contexts from electric circuits to shock absorbers in automobiles to the endocrine system, certain features of nonlinear models have wide applicability. These include period doubling, the ability to reset the phase (timing) of a nonlinear oscillator, and deterministic chaos.

Some have said that Newtonian physics has been overthrown by chaos. This is not true. The same equations hold; predictable motions with which we have long been familiar still take place. Much of our current technology is based on them. We build television sets and send a spacecraft to explore several planets in succession. With chaos, we have come to understand a rich set of solutions to these same equations that we were not equipped to study before.

Many books about nonlinear systems have been written. A particularly interesting one for this audience is by Kaplan and Glass (1995). It is written for biologists and has many clear and relevant examples. Others are by Glass and Mackey (1988), by Hilborn (2000), and by Strogatz (1994).

Space limitations prevent more than a brief hint at some of the features of nonlinear dynamics, here and in Chap. 11. In this section we will discuss some one- and two-dimensional nonlinear differential equations. These will not lead to chaos, but will allow us to describe a very simple model for *phase resetting*. In Sect. 10.9 we will discuss equations that exhibit chaotic behavior.

10.8.1 Describing a Nonlinear System

Suppose that a nonlinear system with N variables can be described by a set of N first-order differential equations:

$$\begin{aligned} \frac{dx_1}{dt} &= f_1(x_1, x_2, \ldots, x_N), \\ \frac{dx_2}{dt} &= f_2(x_1, x_2, \ldots, x_N), \\ &\ldots, \\ \frac{dx_N}{dt} &= f_N(x_1, x_2, \ldots, x_N). \end{aligned} \tag{10.35}$$

(These are an extension of the pair of differential equations we saw as Eqs. 10.27. Our model of breathing had two variables. It would be more realistic to use a breathing model with more variables, since alveolar ventilation also depends on arterial pH, weakly on oxygen partial pressure, and on the nervous factors that were described earlier.)

If the equations are cast in this form with N variables, then N initial conditions are required, corresponding to the constant of integration required for each equation. It is customary to say that there are N *degrees of freedom*. This is the language of *system dynamics*. This definition of degrees of freedom is different from what we used in Chap. 3, where each degree of freedom was represented by a second-order differential equation ($d^2x/dt^2 = F_x/m$, for example) and two initial conditions were required for each degree of freedom.

We can put Newton's second law in this form by writing two first-order differential equations instead of one second-order equation. For motion in one dimension, instead of

$$m\frac{d^2x}{dt^2} = F(x, v),$$

we write a pair of first-order equations:

$$\frac{dv}{dt} = \frac{F(x, v)}{m}, \quad \frac{dx}{dt} = v.$$

This system has two degrees of freedom in our new terminology. In either description, two initial conditions are required.

In many situations the force (or more generally the functions on the right-hand side of Eqs. 10.35) is time dependent. In standard form, the functions on the right do not depend on time. This is remedied by introducing one more variable, $x_{N+1} = t$. The additional differential equation is $dx_{N+1}/dt = 1$.

The evolution or " motion" of the system can be thought of as a trajectory in N-dimensional space, starting from the point that represents the initial conditions. Time is a parameter. We have seen an example of this for two dimensions in Figs. 10.13 and 10.14. It is possible to prove that two distinct trajectories cannot intersect in a finite period of time and that a single trajectory cannot cross itself at a later time (see Hilborn 2000, p. 77 or Strogatz 1994, p. 149). This is true in the full N-dimensional space; if we were to measure only two variables, we could see apparent intersections in the state plane that we were observing. This means that chaotic behavior, in which variables appear to change wildly and two-dimensional trajectories appear to cross, does not occur for a pair of differential equations of the form in Eqs. 10.35. At least three variables are required. A system with two degrees of freedom that is externally driven[2] can

[2] That is, one of the functions on the right-hand side of the set of equations depends on time.

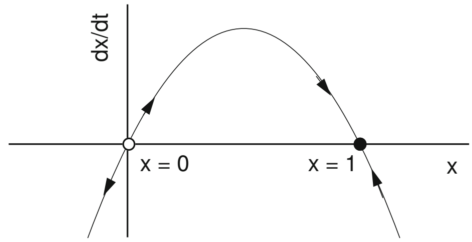

Fig. 10.16 Plot of dx/dt vs. x for the logistic differential equation

exhibit chaotic behavior because of the additional variable x_{N+1} that is introduced.

10.8.2 An Example of Phase Resetting: The Radial Isochron Clock

In Chap. 2 we studied the logistic differential equation

$$\frac{dy}{dt} = by\left(1 - \frac{y}{y_\infty}\right).$$

It is convenient to rewrite the logistic equation in terms of the dimensionless variable $x = y/y_\infty$:

$$\frac{dx}{dt} = bx(1-x). \tag{10.36}$$

This separates the scale factor y_∞ from the dynamic factor b that tells how rapidly y and x are changing.[3] A plot of dx/dt vs. x is shown in Fig. 10.16. There is an unstable fixed point at $x = 0$ and a stable fixed point at $x = 1$. The logistic equation is one of a whole class of nonlinear first-order differential equations for which dx/dt as a function of x has a maximum. It has been studied extensively because of its relative simplicity, and it has been used for population modeling. (Better population models are available.[4] The logistic model assumes that the population is independent of the populations of other species, that the growth of the species does not affect the carrying capacity y_∞, and that the population increases smoothly with time.)

Many of the important features of nonlinear systems do not occur with one degree of freedom. We can make a very simple model system that displays the properties of systems with two degrees of freedom by combining the logistic equation for variable r with an angle variable θ that increases at a constant rate:

$$\frac{dr}{dt} = ar(1-r), \qquad \frac{d\theta}{dt} = 2\pi. \tag{10.37}$$

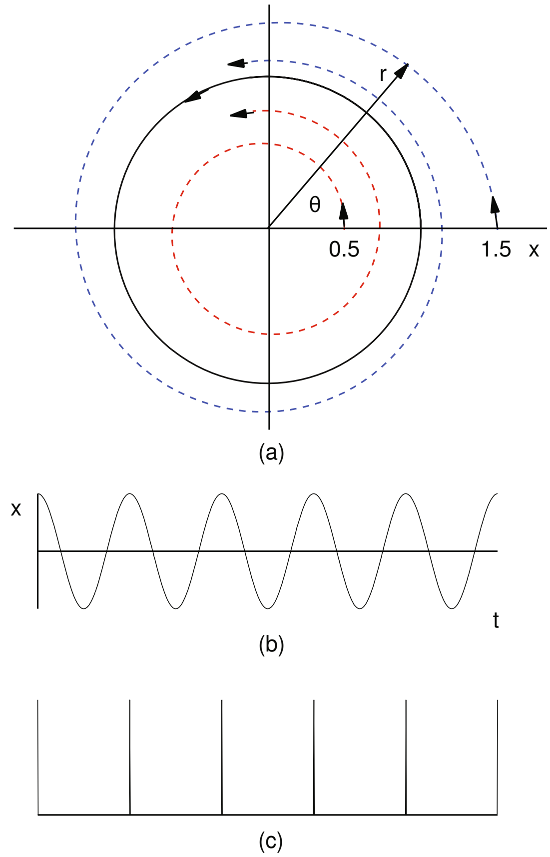

Fig. 10.17 A system with two degrees of freedom. **a** The limit cycle is represented by the solid circle. Systems starting elsewhere in the plane have trajectories that approach the limit cycle as $t \to \infty$, as shown by the dashed lines. **b** The value of $x = r\cos\theta$ is plotted as a function of time. **c** A timing pulse is generated every time θ is a multiple of 2π

We can interpret (r, θ) as the polar coordinates of a point in the xy plane. When t has increased from 0 to 1 the angle has increased from 0 to 2π, which is equivalent to starting again with $\theta = 0$. This model system has been used by many authors. Glass and Mackey (1988) have proposed that it be called the *radial isochron clock*. Typical behavior is shown in Fig. 10.17a. If $r = 1$, there is a circular orbit corresponding to the stable fixed point of Eq. 10.36. Such a stable orbit is called a *stable limit cycle*.[5] There is an unstable limit cycle, $r = 0$, corresponding to the unstable fixed point of Eq. 10.36. Any initial conditions except $r = 0$ give trajectories that move toward the stable circular limit cycle as time progresses. The set of points in the xy plane lying on orbits that move to the limit cycle as $t \to \infty$ is called the *basin of attraction* for the limit cycle. In this case the basin of attraction

[3] We could also, if we wish, define a new time scale, $t' = bt$, and deal with the completely dimensionless equation $dx/dt' = x(1-x)$.

[4] See Begon et al. (1996).

[5] A *stable limit cycle* is an oscillation in the solutions to a set of differential equations that is always reestablished following any small perturbation.

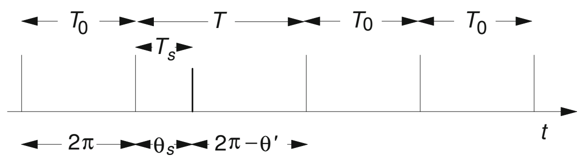

Fig. 10.18 Resetting the phase of an oscillation. The oscillator fires regularly with period T_0. A stimulus at time T_s after it has fired causes a period of length T, after which the periods are again T_0

includes all points except the origin. If we look at the time behavior, Fig. 10.17b shows the behavior of $x = r\cos\theta$ on the limit cycle. The oscillator might provide timing information as the phase moves through some value. Figure 10.17c shows a series of pulses every time θ is a multiple of 2π.

In many cases the differential equations contain one or more parameters that can be varied, and the number and shape of the limit cycles change as the parameters are changed. A point in parameter space at which the number of limit cycles changes or their stability changes is called a *bifurcation*. We will see examples of bifurcations in the next section. See the references for a much more extensive discussion.

One important characteristic of nonlinear oscillators is that a single pulse can reset their phase. If they are subject to a series of periodic pulses they can be *entrained* to oscillate at the driving frequency. (The nonlinear oscillators that sweep the electron beam across the screen of a television tube are entrained by synchronization pulses in the television signal.) Our simple two-dimensional model exhibits phase resetting that is very similar to that exhibited by cardiac tissue.[6]

Suppose that a cardiac pacemaker depolarizes every T_0 seconds and that it can be modeled by our radial isochron clock. Assume that depolarization occurs when $\theta = 0$ or a multiple of 2π. A stimulus is applied at time T_s after the beginning of the cycle, as shown in Fig. 10.18. As a result, the time from the previous depolarization to the next one is changed to T, after which the period reverts to T_0. (In a real experiment, it may be necessary to wait several cycles before measuring so that any transient behavior has time to decay, and then extrapolate back to find the value of T.) Often a stimulus early in the cycle is found to delay the next depolarization, while a stimulus late in the cycle advances it. Our model provides a simple geometric interpretation of this behavior, independent of any knowledge of the detailed dynamics.

[6] This discussion is based on Glass and Mackey (1988), p. 104 ff. See also the works by Winfree (1987, 2001). Strogatz (2003) discusses phase resetting and other nonlinear phenomena in an engaging and nonmathematical manner.

A delayed depolarization is shown in Fig. 10.18. Pulses are occurring every T_0 seconds when the phase is a multiple of 2π (that is, 0). A stimulus is applied at a time T_s after the previous pulse, at which time the phase is θ_s. Since the phase advances linearly, we have the proportion

$$\frac{T_s}{T_0} = \frac{\theta_s}{2\pi}.$$

Suppose the stimulus causes the system to move to a new state with a phase θ', which we do not yet know. Since in our model $d\theta/dt$ is constant, the phase advances after the stimulus at the same rate as it would have without the stimulus. The next pulse occurs when the phase again reaches 2π. This occurs at a time T after the previous pulse, or a time $T - T_s$ after the stimulus, when the phase has increased from θ' to 2π. Therefore

$$\frac{T - T_s}{T_0} = \frac{2\pi - \theta'}{2\pi}$$

and

$$\frac{T}{T_0} = \frac{2\pi + \theta_s - \theta'}{2\pi}. \tag{10.38}$$

We use our limit cycle model to relate θ_s and θ' as shown in Fig. 10.19. The system has been moving on a circle of unit radius representing the stable limit cycle. Assume that the only effect of the stimulus is to shift the value of x by a distance b along the $+x$ axis. For the angles shown in Fig. 10.19a this results in a point with $\theta' < \theta_s$, a delay in the phase or $T > T_0$. For an initial angle in the lower half plane (Fig. 10.19b) it results in $\theta' > \theta_s$ and $T < T_0$. The relation between the two angles can be obtained from the triangles:

$$\begin{aligned}\cos\theta' &= \frac{\cos\theta_s + b}{\left[(\cos\theta_s + b)^2 + \sin^2\theta_s\right]^{1/2}} \\ &= \frac{\cos\theta_s + b}{(1 + b^2 + 2b\cos\theta_s)^{1/2}}.\end{aligned}$$

The stimulus changed both θ and r. After the stimulus each evolves independently according to its own differential equation. The trajectory returns to the limit cycle as r returns to its attractor, but the phase is forever altered. Figure 10.20a is a plot of θ' vs. θ_s for two values of b. When $b < 1$, θ' takes on all values, while for $b > 1$, θ' is restricted to values near 0 and 2π. The first case is called a *type-1 phase resetting*, and the second is called a *type-0 phase resetting*. Figure 10.20b combines these results with Eq. 10.38 to determine T/T_0 as a function of T_s/T_0.

Figure 10.21 shows experimental data for electrotonically stimulated Purkinje fibers from the conduction system of a dog. The fibers were undergoing spontaneous oscillation with $T_0 = 1.575$ s. Stimuli of two different amplitudes were applied at different parts of the cycle, T_s/T_0. Two different curves were obtained. The one with larger current looks like

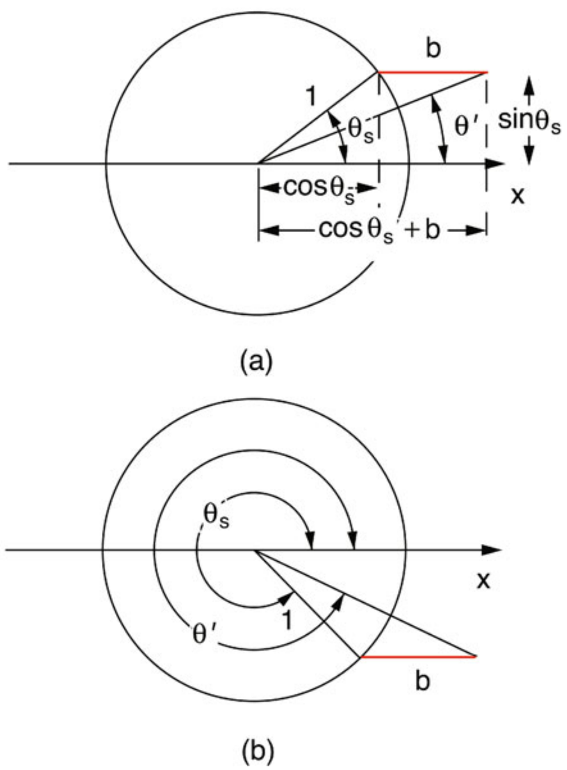

Fig. 10.19 The limit-cycle oscillator model for resetting the phase of an oscillation. At phase θ_s a stimulus changes the value of x by an amount $+b$. **a** For angles $0 < \theta_s < \pi$, this places the system on a trajectory with a smaller phase θ', delaying the next pulse. **b** For angles $\pi < \theta_s < 2\pi$, the stimulus results in a larger phase and the next pulse occurs earlier. The system returns to the limit cycle while θ continues to increase at a constant rate

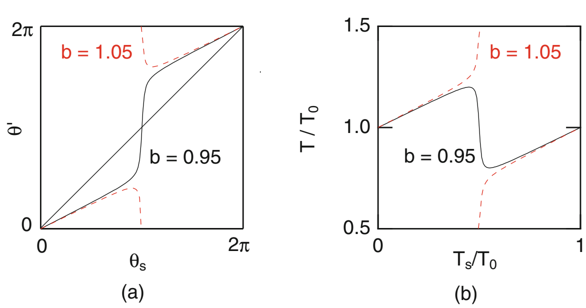

Fig. 10.20 Plots of **a** the new phase vs. the old phase and **b** the length of the period vs. the time when the stimulus is applied

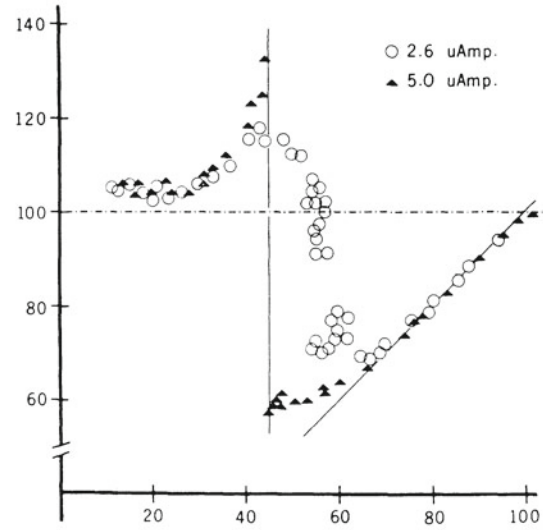

Fig. 10.21 Phase resetting of a spontaneously oscillating Purkinje fiber by stimulation with an electrical impulse. The abscissa is T_s/T_0 expressed as a percentage. The ordinate is T/T_0 expressed as a percentage. Two different stimulus strengths were used. Compare the smaller stimulus (the open circles) to $b = 0.95$ and the larger stimulus (solid triangles) to $b = 1.05$ in Fig. 10.20b. (Reproduced with permission from Jalife and Moe (1976). Copyright 1976 American Heart Association)

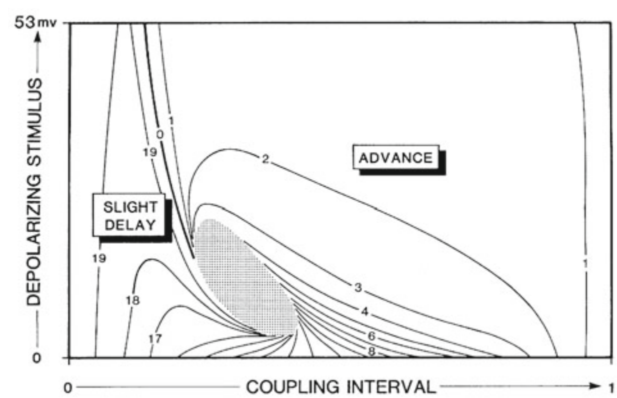

Fig. 10.22 Phase resetting in a Hodgkin–Huxley model. The coupling interval is the delay from the previous pulse to the stimulation pulse in fractions of a period. The ordinate shows the size of the stimulus pulse in mV. The contours show the latency or time from the stimulus to the next pulse, measured in twentieths of a period. (From Winfree (1987). Copyright ©1987. Reproduced by permission of Prof. Arthur Winfree)

the curve with $b = 1.05$ in Fig. 10.20b, while the one with smaller current looks like the curve with $b = 0.95$.

10.8.3 Stopping an Oscillator

It is theoretically possible to apply a stimulus that would put the system at the point $r = 0$ in the state space. In that case it would not oscillate, though for this model $r = 0$ is an unstable equilibrium point and any slight perturbation would lead the system back to the stable limit cycle. In more complicated models it is possible to have a region of state space corresponding to no oscillation and a basin of attraction that leads to it. Figure 10.21 shows the results of a calculation by Winfree (1987) of the effect of stimuli on resetting the phase of the Hodgkin–Huxley equations adjusted to oscillate spontaneously. The abscissa is the coupling interval or the time after the previous pulse at which the stimulus is delivered. The ordinate is the height of the depolarizing pulse in mV. The contour lines show different values of the latency—the time in twentieths of a cycle period from the stimulus to the next pulse. Winfree called the shaded region of state space where annihilation occurs a "black hole."[7]

10.9 Difference Equations and Chaotic Behavior

We have alluded to the possibility of chaotic behavior, but we have not yet seen it. Chaotic behavior of nonlinear differential equations requires three or more degrees of freedom. It is possible to see chaotic behavior in difference equations with a single degree of freedom because the restriction that the trajectory cannot cross itself or another trajectory no longer applies. It arose from the continuous nature of the trajectories for a system of differential equations.

10.9.1 The Logistic Map: Period Doubling and Deterministic Chaos

We considered the logistic differential equation as a model for population growth. The differential equation assumes that the population changes continuously. For some species each generation is distinct, and a difference equation is a better model of the population than a differential equation. An example might be an insect population where one generation lays eggs and dies, and the next year a new generation emerges. A model that has been used for this case is the logistic difference equation or *logistic map*

$$y_{j+1} = a y_j \left(1 - \frac{y_j}{y_\infty}\right)$$

with $a > 0$ and j the generation number. It can again be cast in dimensionless form by defining $x_j = y_j / y_\infty$:

$$x_{j+1} = a x_j (1 - x_j). \tag{10.39}$$

While superficially this looks like the logistic differential equation, it leads to very different behavior. The stable points are not even the same. A plot of x_{j+1} vs. x_j is a parabola,

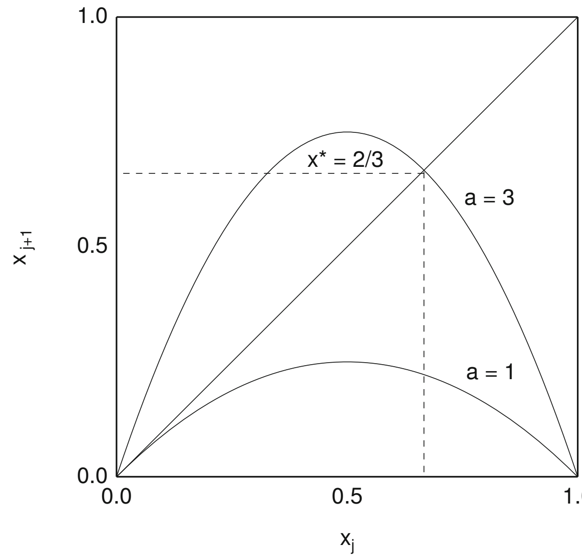

Fig. 10.23 Plot of x_{j+1} vs. x_j for the logistic difference equation or logistic map, for two values of parameter a

from which we can immediately see the following properties of the logistic map:

$$\begin{aligned} x_j &< 0, & x_{j+1} &< 0, \\ x_j &= 0, & x_{j+1} &= 0, \\ 0 < x_j &< 1, & x_{j+1} &> 0, \\ x_j &= 1, & x_{j+1} &= 0, \\ x_j &> 1, & x_{j+1} &< 0. \end{aligned}$$

If we are to use this as a population model, we must restrict x to values between 0 and 1 so the values do not go to $-\infty$. In order to keep successive values of the map within the interval (0, 1) we also make the restriction $a < 4$.

For the logistic differential equation, $x = 1$ was a point of stable equilibrium. However, for the logistic map, if $x_j = 1$ the next value is $x_{j+1} = 0$. The equilibrium value x^* can be obtained by solving Eq. 10.39 with $x_{j+1} = x_j = x^*$:

$$x^* = a x^* (1 - x^*) = 1 - 1/a. \tag{10.40}$$

Point x^* can be interpreted graphically as the intersection of Eq. 10.39 with the equation $x_{j+1} = x_j$ as shown in Fig. 10.23. You can see from either the graph or from Eq. 10.40 that there is no solution for positive x if $a < 1$. For $a = 1$ the solution occurs at $x^* = 0$. For $a = 3$ the equilibrium solution is $x^* = 2/3$. Figure 10.24 shows how, for $a = 2.9$ and an initial value $x_0 = 0.2$, the values of x_j approach the equilibrium value $x^* = 0.655$. This equilibrium point is called an *attractor*.

[7] See Winfree (1987), especially Chaps. 3 and 4, or Glass and Mackey (1988), pp. 93–97.

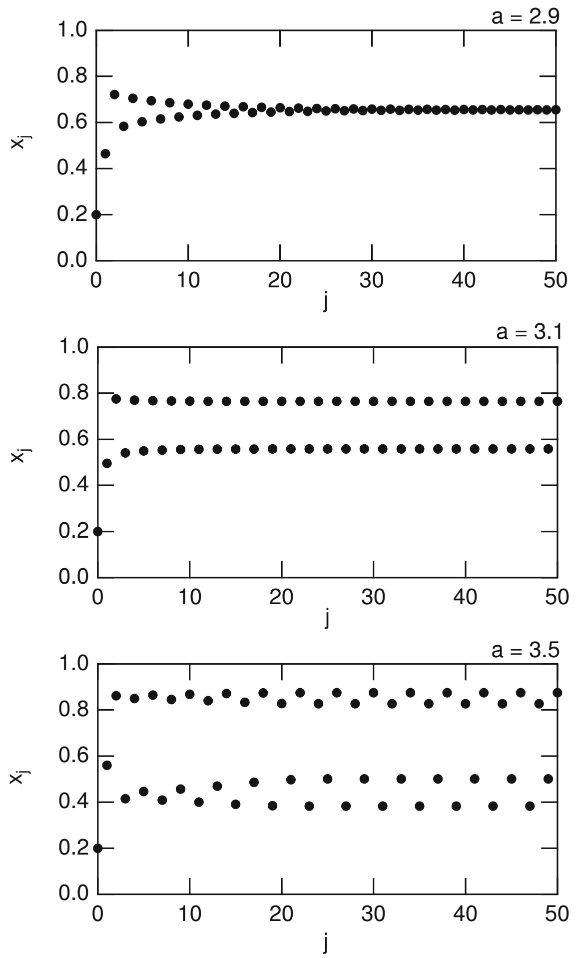

Fig. 10.24 Plots of x_j vs. j for different values of a, showing how the sequence of values converges to one, two, or four values of x called the *attractors*

Figure 10.24 also shows the remarkable behavior that results when a is increased to 3.1. The values of x_j do not come to equilibrium. Rather, they oscillate about the former equilibrium value, taking on first a larger value and then a smaller value. This is called a *period-2 cycle*. The behavior of the map has undergone *period doubling*. What is different about this value of a? Nothing looks strange about Fig. 10.23. But it turns out that if we consider the slope of the graph of x_{j+1} vs. x_j at x^*, we find that for $a > 3$ the slope of the curve at the intersection has a magnitude greater than 1. Many books explore the implications of this.

The period doubling continues with increasing a. For $a > 3.449$ there is a cycle of period 4. A plot of the period-4 cycle for $a = 3.5$ is also shown in Fig. 10.24. For $a > 3.54409$ there is a cycle of period 8. The period doubling continues, with periods 2^N occurring at more and more closely spaced values of a. When $a > 3.569946$, for many values of a the behavior is aperiodic, and the values of x_j never form a repeating sequence. Remarkably, there are ranges of a in this

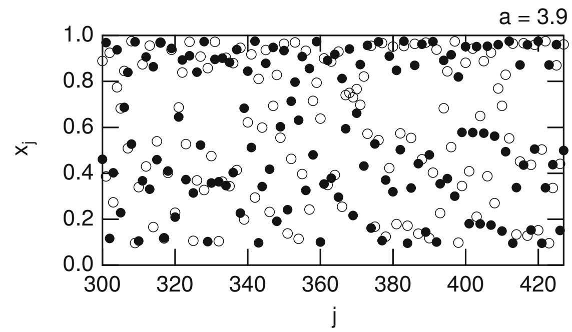

Fig. 10.25 For this value of a the solution is aperiodic. There is no attractor

region for which a repeating sequence again occurs, but they are very narrow. The details of this behavior are found in many texts. In the context of ecology they are reviewed in a classic paper by May (1976).

For $a < 3.569946$, starting from different initial values x_0 leads after a number of iterations to the same set of values for the x_j. For values of a larger than this, starting from slightly different values of x_0 usually leads to very different values of x_j, and the differences become greater and greater for larger values of j. This is shown in Fig. 10.25 for $a = 3.9$. The sequence is plotted from $j = 301$ to $j = 425$. The solid circles represent the sequence starting with $x_0 = 0.20$; the open circles represent the sequence for $x_0 = 0.21$.

This is an example of chaotic behavior or *deterministic chaos*. Deterministic chaos has four important characteristics:

1. The system is deterministic, governed by a set of equations that define the evolution of the system.
2. The behavior is bounded. It does not go off to infinity.
3. The behavior of the variables is aperiodic in the chaotic regime. The values never repeat.
4. The behavior depends very sensitively on the initial conditions.

10.9.2 The Bifurcation Diagram

Figure 10.26 shows the values of x_j that occur after any transients have died away for different values of parameter a. The diagram was made by picking a value of a. A value of x_0 was selected and the iterations were made. After 50 iterations, the next 300 values of x_j were plotted. Then a was incremented slightly and the process was repeated. This is called a *bifurcation diagram*. The figure shows the range $1 < a < 4$. The asymptotic value of x_j rises according to $x^* = 1 - 1/a$ until period doubling occurs at $a = 3$. A four-cycle appears for $a > 3.449$, and for $a > 3.569946$ chaos sets in. Within the chaotic region are very narrow bands of finite periodicity.

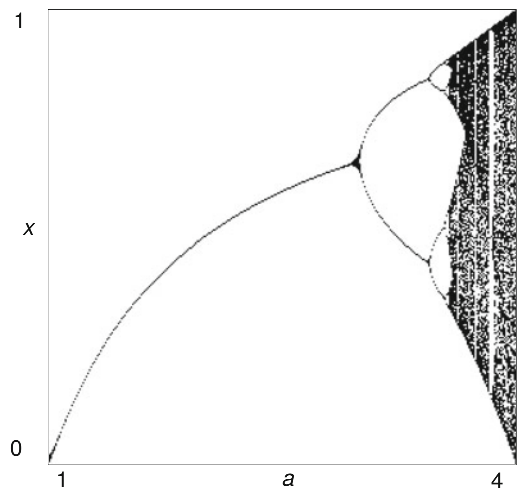

Fig. 10.26 A bifurcation diagram for the logistic map, showing 300 values of x_j for values of a between 1 and 4. The plot was made using the Macintosh software *A Dimension of Chaos* by Matthew A. Hall.

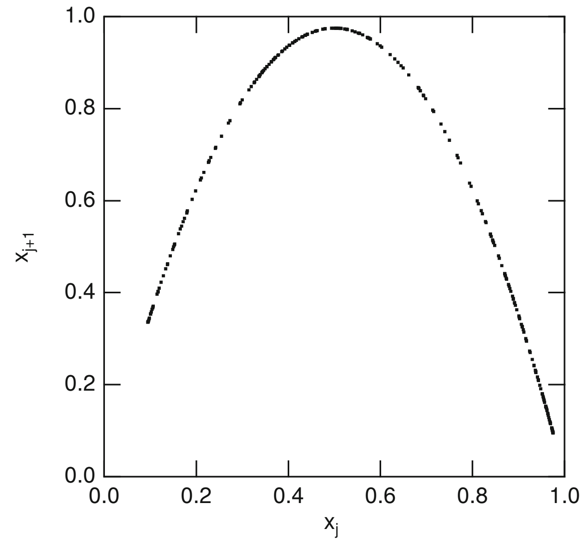

Fig. 10.28 A plot of x_{j+1} vs x_j for the data of Fig. 10.25 recovers the logistic map

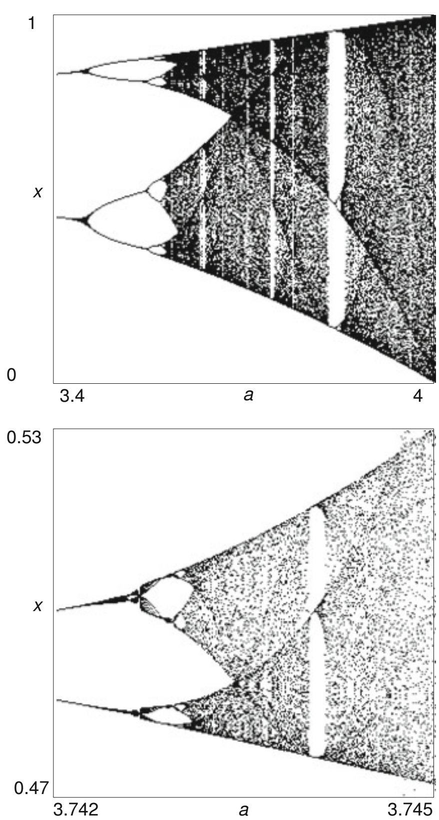

Fig. 10.27 An example of self-similarity. The top curve shows $3.4 < a < 4$. The bottom curve shows $3.742 < a < 3.745$. Note its similarity to the top curve. The plot was made using the Macintosh software *A Dimension of Chaos* by Matthew A. Hall

Figure 10.27 shows a feature of many chaotic systems called *self-similarity*. The bifurcation diagram is plotted for two ranges of a: 3.4–4.0 and 3.743–3.745. The x scale is expanded in the second diagram. Note the similarity of the two bifurcation diagrams.

Even though the plot of x_j vs. j in Fig. 10.25 has no obvious pattern, the values of x_j were obtained from the logistic map. When we plot x_{j+1} vs. x_j the points fall on the map (Fig. 10.28).

The simplest systems in which chaotic behavior can be seen are first-order difference equations in which x_{j+1} is a function of x_j. The function is peaked and "tunable" by some parameter. Chaotic behavior occurs for some values of the parameter. In fact, it appears that the ratios of the parameter values involved in the period doubling and approach to chaos may be independent of the particular shape of the curve.[8]

10.9.3 Quasiperiodicity

Some systems exhibit *quasiperiodicity*. Consider the map $x_{j+1} = x_j + b$ where b is a fixed parameter. Wrap the function back on itself so that x remains in the interval (0, 1). This is done by using the modulo or remainder function.[9] The map is

$$x_{j+1} = x_j + b \,(\mathrm{mod}\, 1)\,. \tag{10.41}$$

[8] See Hilborn (1995), Chap. 2, Kaplan and Glass (1995), p. 30, or Strogatz (1994), p. 370.

[9] The function $x \bmod n$ gives the number that remains after subtracting n from x enough times so that the result is less than 1. For example, $1.5742 \bmod 1 = 0.5742$; $7.5 \bmod 1 = 0.5$.

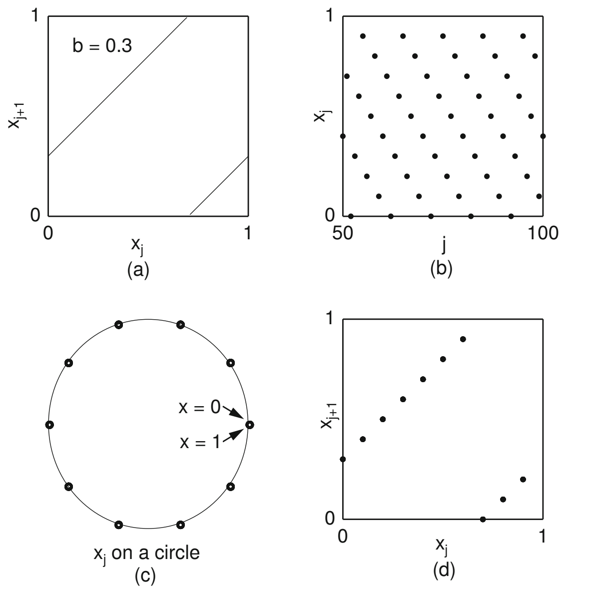

Fig. 10.29 The linear map $x_{j+1} = x_j + 0.3 \pmod 1$. **a** Plot of the map. **b** Plot of x_j vs. j for 50 points. **c** The map plotted on a *circle* for 128 values of j, which lie on only 10 points. **d** A plot of 128 values of x_{j+1} vs. x_j falls on 10 points on the map

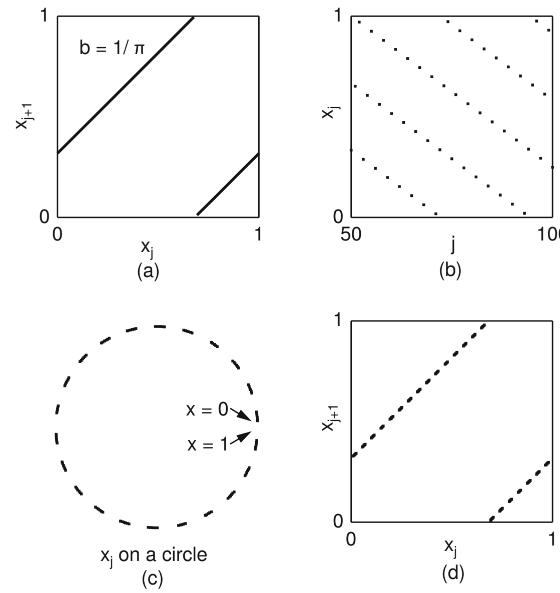

Fig. 10.30 The linear map $x_{j+1} = x_j + 1/\pi \pmod 1$. **a** Plot of the map. **b** Plot of x_j vs j for 50 points. **c** The map plotted on a *circle* for 128 points. **d** Plot of x_{j+1} vs. x_j gives 128 points on the map

The function is plotted in Fig. 10.29 for $b = 0.3$. The map is plotted in (a). The apparent discontinuities are due to the wrapping. A sequence of 50 points is plotted in Fig. 10.29b. Because $b = 3/10$ is a rational fraction, the points repeat themselves exactly every 10 steps. This can be seen in Fig. 10.29c, which plots 128 consecutive points on a circle. The angle counterclockwise from the horizontal axis is $\theta_j = 2\pi x_j$. The 128 values all fall at 10 points on the circle. The plot of x_{j+1} vs. x_j in Fig. 10.29d has 10 points that fall on the map.

Compare this with Fig. 10.30, which is a plot of the same map for an irrational value of the parameter, $b = 1/\pi$. The curve in Fig. 10.30a looks very similar. However, the values of x_j never repeat. This is difficult to see from Fig. 10.30b, but can be seen in c, where the 128 points are all at different values of θ. If more points were plotted, the circle would be completely filled. All of the points plotted in d are also different, but of course they lie on the map function. If we were to make a bifurcation diagram the values of x_j would fill all points on the graph, unless b were a rational fraction, when there would be a finite number of points. This appears at first sight to be chaotic behavior, but it is not. The function is deterministic, it is bounded, and the values of x never repeat. But it does not satisfy the last criterion: sensitive dependence on initial conditions. In chaotic behavior, two trajectories that start from initial points that are very close diverge in time. If a slightly different value of x_0 is used for this map, all of the values in the new sequence are shifted from the original sequence by the same amount. There is no divergence of the two solutions. In quasiperiodicity, the trajectories for two points that are initially close remain close.

10.10 A Feedback Loop with a Time Constant and a Fixed Delay

In Sect. 10.6 we saw that if both processes in a two-stage feedback system had comparable time constants, there was the possibility for damped oscillations or "ringing." Another possibility is that a portion of the system may respond to values of a state variable at some earlier time. The fixed time delay could be the time it takes a signal to travel along a nerve or the time it takes for a chemical to pass through a blood vessel.

We will consider a linear model for such a system, as shown in Fig. 10.31:

$$\begin{aligned} \tau_1 \frac{dy}{dt} + y &= G_1 x + p_1, \\ x &= G_2 y(t - t_d) + p_2. \end{aligned} \tag{10.42}$$

The first equation is like those in Sect. 10.6, except that the factor a multiplying p_1 is set equal to unity. The second equation says that $x(t)$ is proportional to the value of y at

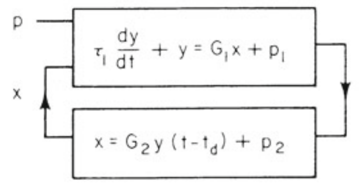

Fig. 10.31 A two-stage feedback loop. The upper process is described by a single time constant; the lower one introduces a fixed time delay

the earlier time $t - t_d$, plus some other parameter p_2. These can be combined to give a *delay-differential equation*:

$$\tau_1 \frac{dy}{dt} = -y + G_1 G_2 y(t - t_d) + p_1 + G_1 p_2$$

or, defining $p = p_1 + G_1 p_2$ to eliminate clutter,

$$\tau_1 \frac{dy}{dt} = -y + G_1 G_2 y(t - t_d) + p. \qquad (10.43)$$

This equation can give rise to sustained as well as damped oscillations. It is not hard to see why. Suppose that y is above some equilibrium value and that $G_1 G_2 < 0$. The first term on the right causes y to decrease toward equilibrium. But when it is nearly at equilibrium the second term, responding to an earlier positive value of y, continues to make y decrease so y goes negative. Now y is below the equilibrium value and the same arguments can be applied as y increases. This paragraph could go on for a long time.

Why do we now have oscillations for a system with apparently only one degree of freedom? The reason is the delay term. In order to specify the initial state of the system at $t = 0$, we must specify the value of y for all times $-t_d < t < 0$. This is effectively an infinite number of values of y. Delay differential equations have an infinite number of degrees of freedom.

The mathematics for such a system become quite involved (even for the linear system we discuss here). The techniques for solving the equation were first described by Hayes (1950). The equation has been considered for biological examples by Glass and Mackey (1988).

The derivative is zero and the equation has a fixed point y_f when $y_f = p/(1 - G_1 G_2)$. It is convenient to work with the new variable $w = y - y_f$ and rewrite Eq. 10.43 as

$$\tau_1 \frac{dw}{dt} = -w + G_1 G_2 w(t - t_d).$$

We make another simplifying assumption; that the magnitude of the open-loop gain $G_1 G_2$ is so much greater than 1 that the $-w$ term can be neglected.[10] Then the equation becomes

$$\frac{dw}{dt} = \frac{G_1 G_2}{\tau_1} w(t - t_d).$$

Now recall that since $G_1 G_2 \ll -1$, this coefficient is approximately the negative of the reciprocal of the time constant with no delay and *with* feedback (see Eq. 10.23). Therefore the equation we will solve is

$$\frac{dw}{dt} = -\frac{1}{\tau} w(t - t_d). \qquad (10.44)$$

If the delay time is zero, this is the familiar equation for exponential decay. As we argued above, a delay can allow oscillation. One can show by substitution that for certain values of the parameters one possible solution has the form $w(t) = w_0 e^{-\gamma t} \cos \omega t$. We will find the conditions for a steady oscillation of the form $w(t) = w_0 \cos \omega t$. The left-hand side of Eq. 10.44 is $dw/dt = -\omega w_0 \sin \omega t$. The right-hand side is

$$\begin{aligned} -(1/\tau) w_0 \cos(\omega t - \omega t_d) &= -(1/\tau) w_0 \cos \omega t \cos \omega t_d \\ &\quad - (1/\tau) w_0 \sin \omega t \sin \omega t_d. \end{aligned}$$

Therefore the proposed solution will satisfy Eq. 10.44 only if

$$-\omega w_0 \sin \omega t = -(1/\tau) w_0 \sin \omega t_d \sin \omega t$$

and

$$0 = -(1/\tau) w_0 \cos \omega t_d \cos \omega t,$$

from which we get $\omega = 1/\tau$ and $\cos \omega t_d = 0$ or $\omega t_d = \pi/2$. Combining these gives $t_d/\tau = \pi/2$. From these we see exactly how the sustained oscillation occurs. The delay time and frequency are such that the shift is exactly one-quarter cycle. This is the same shift that would be obtained by taking the second time derivative of the undelayed function, which would lead to the undamped harmonic oscillator equation.

10.11 Negative Feedback Loops: A Summary

The last several sections have been mathematically complex. However, you do not need to memorize a large number of equations to carry away the heart of what is in them. The essential features are as follows:

1. If the equations relating the input and output variables of each process of a negative feedback loop are known, then their simultaneous solution gives the equilibrium or steady-state values of the variables. (In a biological system it may be very difficult to get these equations.) The

[10] If you are considering a problem where this is not a reasonable assumption, see the Appendix of Glass and Mackey (1988).

solution is called the operating point or a fixed point of the system of equations.
2. If a single process in the negative feedback loop determines the time behavior, and the rate of return of a variable to equilibrium is proportional to the distance of that variable from equilibrium, then the return to equilibrium is an exponential decay and the system can be characterized by a time constant.
3. In a negative feedback system one variable changes to stabilize another variable. The amount of stabilization and the accompanying decrease in time constant depend on the open-loop gain.
4. It is possible to have oscillatory behavior with damped or constant amplitude if the two processes have comparable time constants and sufficient open-loop gain, or if one of the processes depends on the value of its input variable at an earlier time, or if the process has three or more degrees of freedom.
5. A nonlinear system oscillating on a limit cycle can have its phase reset by an external stimulus.
6. Nonlinear systems of difference equations with one or more degrees of freedom or nonlinear systems of differential equations with three or more degrees of freedom may exhibit bifurcations and chaotic behavior.

10.12 Additional Examples

This section provides some additional examples of the principles we have seen above. The details of the experiments and modeling are given in the references.

10.12.1 Cheyne–Stokes Respiration

We have seen how the body responds to CO_2 levels in the blood by controlling the rate and amplitude of breathing to maintain the CO_2 concentration within a narrow range. The frequency and amplitude of breathing can also undergo oscillation. Some patients almost stop breathing for a minute or so and then breathe with much greater amplitude than normal. This is called *Cheyne–Stokes breathing*. Guyton et al. (1956) showed that diverting carotid artery blood in dogs through a long length of tubing increased the transit time between heart and brain and caused Cheyne–Stokes respirations. Cheyne–Stokes respirations have been modeled with a nonlinear delay-differential equation by Mackey and Glass (1977). Their results are shown in Fig. 10.32.

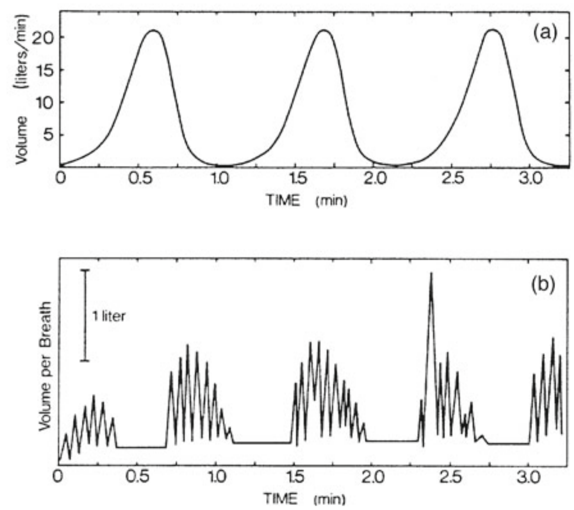

Fig. 10.32 Cheyne–Stokes respirations. **a** The results of the model calculation $y = g(x(t - t_d))$. **b** Ventilation during Cheyne–Stokes respiration. (Reprinted with permission from Mackey and Glass 1977. Copyright 1977 AAAS)

10.12.2 Hot Tubs and Heat Stroke

Problems 10.10 and 10.11 discuss how the body perspires in order to prevent increases in body temperature. At the same time blood flows through vessels near the surface of the skin, giving the flushed appearance of an overheated person. The cooling comes from the evaporation of the perspiration from the skin. If the perspiration cannot evaporate or is wiped off, the feedback loop is broken and the cooling does not occur. If a subject in a hot tub overheats, the same blood flow pattern and perspiration occur, but now heat flows into the body from the hot water in the tub. The feedback has become positive instead of negative, and heat stroke and possibly death occurs. This has been described in the physics literature by Bartlett and Braun (1983).

10.12.3 Pupil Size

The pupil changes diameter in response to the amount of light entering the eye. This is one of the most easily studied feedback systems in the body, because it is possible to break the loop and to change the gain of the system. Let the variables be as follows: x is the amount of light striking the retina, p is the light intensity, and y the pupil area. In the normal case, x is proportional to y and p: $x = Apy$. The body responds to increasing x by decreasing y so $y = f(x)$. These processes are shown in Fig. 10.33.

The reason this system can be studied so easily is that shining a very narrow beam of light into the pupil means that the change of pupil radius no longer affects x; the loop is

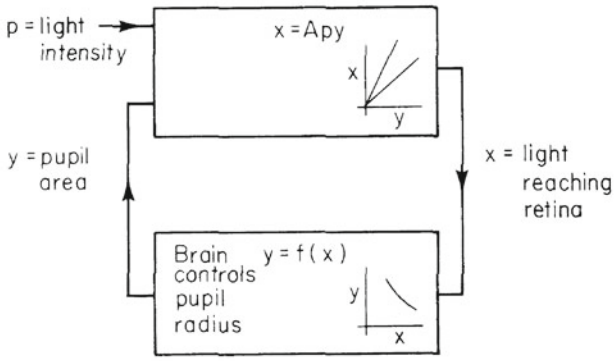

Fig. 10.33 The feedback system for controlling the size of the pupil

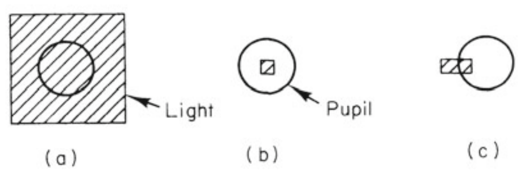

Fig. 10.34 The feedback loop for pupil size can be changed by changing the way in which light strikes the eye. **a** In the normal situation $x = Apy$. **b** When the spot of light is smaller than the pupil, the feedback loop is broken. **c** When the spot of light strikes the edge of the pupil, the gain is increased

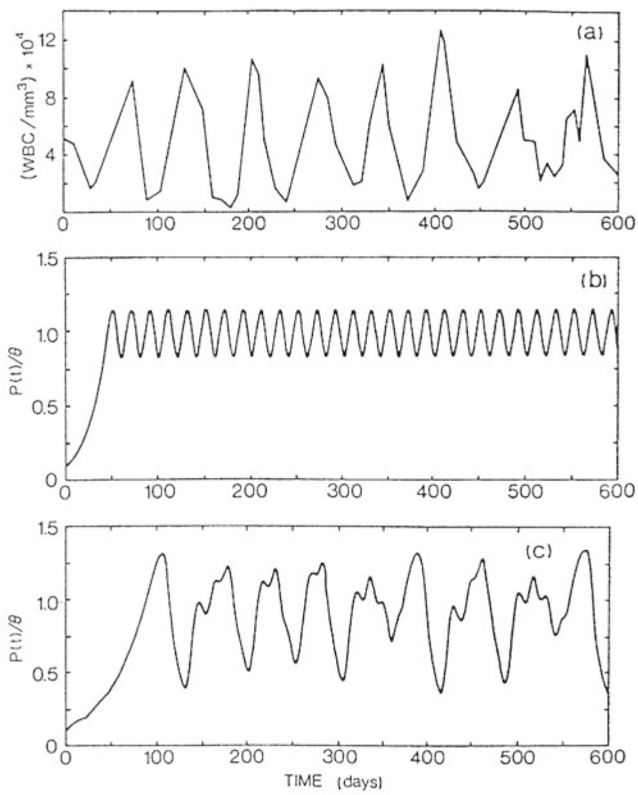

Fig. 10.35 A nonlinear model for white-blood-cell production. **a** White-blood-cell count from a patient with chronic granulocytic leukemia. **b** The results of a nonlinear delay-differential equation model with a delay time of 6 days are an oscillation with a period of 20 days. **c** The results of using the same model with a delay time of 20 days are aperiodic. (Reprinted with permission from Mackey and Glass 1977. Copyright 1977 AAAS)

broken in the upper box of Fig. 10.33. Shining a light into the eye so that it is on the edge of the pupil increases the gain in the upper box. These schemes are shown in Fig. 10.34. Furthermore, it has been discovered experimentally that the process in the lower box controls the size of both pupils, even though light is directed at only one eye.

The properties of $y = f(x)$ have been studied extensively by Stark (see Stark 1957, 1968, 1984). The results are consistent with a feedback loop having several time constants and also a fixed delay. Increasing the open-loop gain as in Fig. 10.34c causes the pupil to oscillate at a frequency of about 1.3 Hz (cycles per second). Stark (1984) reviews this work, including the use of noise to analyze the system and nonlinearities.

10.12.4 Oscillating White-Blood-Cell Counts

A delay-differential equation has been used to model the production of red and white blood cells. Figure 10.35 shows the actual white count for a patient with chronic granulocytic leukemia as well as the results of a model calculation. The striking feature of the model is the emergence of an aperiodic pattern when the delay time is increased from 6 to 20 days.

10.12.5 Waves in Excitable Media

The propagation of an action potential is one example of the propagation of a wave in excitable media. We saw in Chap. 7 that waves of depolarization sweep through cardiac tissue. The circulation of a wave of contraction in a ring of cardiac tissue was demonstrated by Mines in 1914. It was first thought that such a wave had to circulate around an anatomic obstacle, but it is now recognized that no obstacle is needed.

Waves in thin slices of cardiac tissue often have the shape of spirals, very similar to simulations produced by a model similar to a two-dimensional Hodgkin–Huxley model (Gray 2009). These waves occur in many contexts beside the heart. They have also been seen in the Belousov–Zhabotinsky

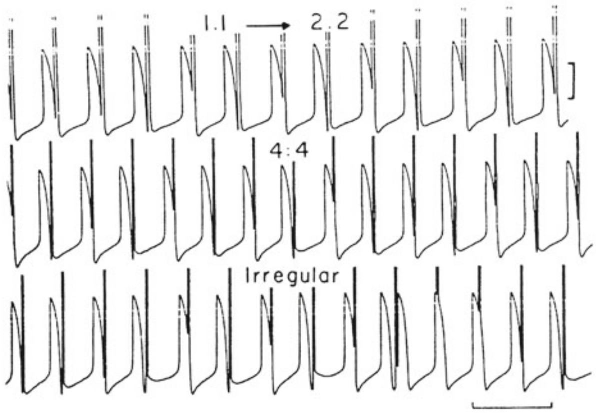

Fig. 10.36 An aggregate of chick heart cells was periodically stimulated. Follow the bottom of the beginning of each sharp spike. The left part of the top strip shows phase locking. The right-hand portion of the top strip shows period doubling. The middle strip shows a period-4 behavior. The bottom strip shows irregular behavior consistent with deterministic chaos. (Reprinted with permission from Guevara et al. 1981. Copyright 1981 AAAS)

chemical reaction,[11] in social amoebae, in the retina of the eye, and as calcium waves in oocytes. Beautiful photographs of all of these are found in Winfree (1987). A simple reaction–diffusion model that leads to a propagating chemical wave is found in Problem 4.28

These *spiral waves* seem to be another ubiquitous phenomenon (like period doubling) that depends primarily on the coarse features of the model. They can be generated with simple computer models called *cellular automata*. The rules for such an automaton and photographs of the resulting spiral waves are shown in Chap. 2 of Kaplan and Glass (1995).

The study of spiral waves in the heart is currently an active field (Glass et al. 2002; Keener and Sneyd 2008a; Panfilov 2009; Gray 2009; Luther et al. 2011; Clayton et al. (2011)). They can lead to ventricular tachycardia, they can meander, much as a tornado does, and their breakup into a pattern resembling turbulence is a possible mechanism for the development of ventricular fibrillation (see the next example).

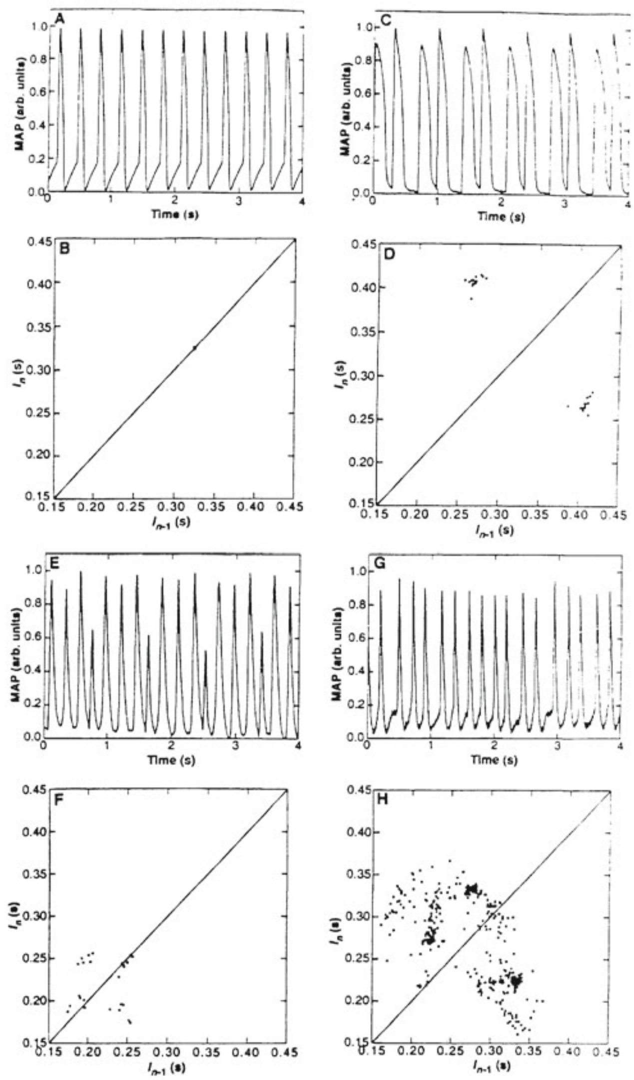

Fig. 10.37 The results of experiments on a preparation consisting of intraventricular septum from a rabbit heart. Plots show the recorded action potentials and the map of I_n vs. I_{n-1} where I is the interval between beats. In *A* and *B* there is a constant interbeat interval and one point on the map. Panels *C* and *D* show period doubling. Panels *E* and *F* show a period-4 pattern. Panels *G* and *H* are completely aperiodic. (Reprinted with permission from Garfinkel et al. 1992. Copyright 1992 AAAS)

10.12.6 Period Doubling and Chaos in Heart Cells

Guevara et al. (1981) have subjected small aggregates of chick heart cells to periodic stimulation. The stimulation frequency was slightly greater than the natural frequency of oscillation. The behavior of the preparation is shown in Fig. 10.36 and can best be seen by examining the *bottom* of the leading edge of the sharp positive pulse. The top strip on the left is phase locking. This is followed on the right in the top strip by an alternation characteristic of period doubling. The middle strip shows a variation of period 4. The bottom strip shows irregularity that is consistent with deterministic chaos.

Garfinkel et al. (1992) have also observed period doubling in a stimulated preparation of rabbit heart. Arrhythmias were induced by adding drugs to the solution perfusing the preparation. Figure 10.37 shows plots of the recorded action potentials and a plot of the map of I_n vs. I_{n-1}, where I is the interval between beats. In panels A and B there is a constant

[11] There are many references. See Mielczarek et al. (1983); Epstein et al. (1983); and Winfree (1987).

interbeat interval and one point on the map. Panels C and D show period doubling. Panels E and F show a period-4 pattern. Panels G and H are completely aperiodic.

Ventricular fibrillation is "the rapid, disorganized, and asynchronous contraction of ventricular muscle. ... it represents the final common pathway for death in most patients who experience out-of-hospital cardiac arrest, and its rate of recurrence is on the order of 30 % in the first year in successfully resuscitated patients." (Epstein and Ideker 1995). It appears to be due to meandering waves, and it does not occur unless the heart exceeds some minimum size (Winfree 2001).

Witkowski et al. (1993, 1994) have made electrode arrays with a spacing of about 200 µm that can be placed directly on the myocardium. The membrane current i_m can be estimated from the spatial derivatives of the extracellular (interstitial) potential. This technique has provided evidence that ventricular fibrillation has a component with simpler dynamics than had previously been thought (Witkowski et al. 1995). More recent studies point toward more complex behavior (Fox et al. 2002).

Symbols Used in Chapter 10

Symbol	Use	Units	First used page
a, b	Arbitrary parameter		277
a	Parameter in logistic map		284
a, b	Constant in logistic equation		281
b	Reduction in ventilation rate because of dead space in lungs	$\mathrm{l\ min^{-1}}$	271
b	Amplitude of stimulus		282
f, g, h, i	Functions		271
j	Index for successive values in difference equation		284
m	Mass	kg	280
n	Number of moles of dissolved carbon dioxide		273
o	Rate of oxygen consumption	$\mathrm{mol\ s^{-1}}$	270
p	Rate of oxygen consumption	$\mathrm{mmol\ min^{-1}}$	270
p	Light intensity		289
r	Variable		281
t	Time	s	273
t_d	Delay time	s	288
v	Velocity	$\mathrm{m\ s^{-1}}$	280
w, x, y, z	General variables		271
x, y	General variables in a feedback system		269
x	Partial pressure of carbon dioxide	torr	270
x	Amount of light striking the retina		289
x^*	Equilibrium value of x		284
y	Ventilation rate	$\mathrm{l\ min^{-1}}$	270
y	Pupil area	$\mathrm{m^2}$	289
y_∞	Constant (carrying capacity) in logistic equation		281
A	Proportionality constant		273
F	Respiratory quotient		270
F	General function		271
F_x	x component of force	N	280
G_1, G_2	Gain		272
I	Interbeat interval	s	291
N	Number of variables		280
P_{CO_2}	Partial pressure of carbon dioxide	torr	270
R	Gas constant	$\mathrm{J\ K^{-1}\ mol^{-1}}$	270
T	Temperature	K	270
T, T_0, T_s	Time	s	282
V_c	Compartment in which carbon dioxide is distributed throughout the body	$\mathrm{m^3}$ or l	273
α	Solubility constant	$\mathrm{mol\ l^{-1}\ torr^{-1}}$	273
α	Damping constant	$\mathrm{s^{-1}}$	277
$\theta, \theta', \theta_s$	Angle		281
τ, τ_1, τ_2	Time constant	s	273
ω, ω_0	Angular frequency	$\mathrm{radian\ s^{-1}}$	277
ξ, η	Variables		273

Problems

Section 10.1

Problem 1. Make the unit conversions to show that Eq. 10.4 is equivalent to Eq. 10.1.

Section 10.2

Problem 2. The level of the thyroid hormone thyroxine (T4) in the blood is regulated by a feedback system. TSH is released by the pituitary. The thyroid responds to increased levels of TSH by producing more T4. The T4 then acts through the hypothalamus and pituitary to reduce the amount of TSH.

(a) On a graph of T4 vs. TSH, plot hypothetical curves showing these two processes and indicate the equilibrium or operating point.

(b) T4 contains four iodine atoms. If the body has an insufficient supply of dietary iodine, the thyroid cannot make enough T4. What changes in the graphs will result? (This causes iodine deficiency goiter or thyroid hyperplasia. With the advent of iodized table salt and the use of iodine by bakers in bread dough to make their equipment easier to clean, the disease has almost disappeared.)

Problem 3. For the feedback system $x = \left[(y-p)/3\right]^{1/2}$, $y = 4 - x^2$ assume that the variable on the right in each equation controls the variable on the left.

(a) Plot y vs. x for each process.
(b) Find the operating point when $p = 0$.
(c) Find the operating point when $p = 1$.

Section 10.3

Problem 4. Find the open-loop gain for the system described in Problem 10.3.

Problem 5. Find the open-loop gain for the system shown.

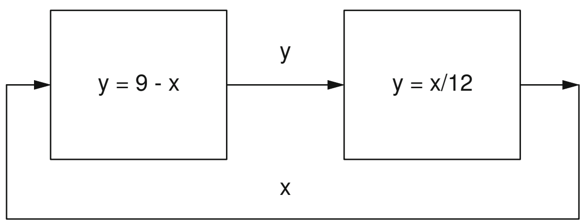

Problem 6. A feedback loop has the three stages shown. Find the operating point and the open-loop gain if these variables are all positive.

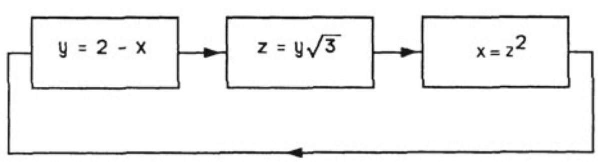

Problem 7. Consider how thyroid hormone is removed from the body by the kidneys. The variables are V, the total plasma volume (l); C, the plasma concentration of thyroid hormone (mol l^{-1}); y, the total amount of hormone (mol); and R, the rate of hormone production (mol s^{-1}). The rate of change is $dy/dt = R - KC$. In the steady state $R = KC$, and y is not changing with time (see Chap. 2). The clearance K is a measure of the kidneys' ability to remove hormone, since the removal process depends on the concentration.

(a) Plot K vs. C for two different values of R. Show on your graph what happens if K remains fixed as R changes.
(b) It has been found experimentally (Riggs 1952. *Pharmacol Rev* **4**: 284–370) that K increases as C increases: $K = aC$. Plot this on your graph, too.
(c) Draw a block diagram showing the proper cause and effect relationship between C and K.
(d) Calculate the open-loop gain. Show how changes in C are altered by the feedback mechanism.

Problem 8. A substance is produced in the body and removed at rate R. The concentration is C. The clearance is defined to be K. In the steady state $0 = dy/dt = R - KC$, or $K = R/C$. It is found experimentally that the clearance depends on the concentration as $K = aC^n$, where C is the independent variable. Find the open-loop gain, eliminating K and a from your answer.

Problem 9. The kidney excretes phosphate in the following way. The total plasma volume V_p contains phosphate at concentration C_p: $Q_p = C_p V_p$. A volume of plasma $(dV/dt)_f$ is filtered through the renal glomeruli into the nephrons each second. Within the nephron, phosphate is either reabsorbed into the plasma or excreted into the urine. Experiments show that virtually all phosphate is reabsorbed up to some rate $(dQ/dt)_{\max}$:

$$\left(\frac{dQ}{dt}\right)_{\text{reabs}} = \begin{cases} C_p\,(dV/dt)_f\,, & C_p\,(dV/dt)_f < (dQ/dt)_{\max} \\ (dQ/dt)_{\max}\,, & C_p\,(dV/dt)_f \geq (dQ/dt)_{\max}\,. \end{cases}$$

As in Problem 7a, at equilibrium the clearance of phosphate from the plasma is defined as

$$K = \frac{(dQ/dt)_{\text{excreted into urine}}}{C_p}.$$

Suppose that exogenous phosphate is entering the plasma at a fixed rate R and that steady state has been reached so that $R = (dQ/dt)_{\text{excreted into urine}}$.

(a) What value for reabsorption does this imply?
(b) Determine two equations relating K and C_p and plot them.
(c) Calculate the open-loop gain of the feedback loop.

Problem 10. With considerable simplification, consider the body to have a constant temperature T throughout and a total heat capacity C. The total amount of thermal energy in the body is U. The heat capacity is defined so that $dU = CdT$. The source of the thermal energy is the body's metabolism: $(dU/dt)_{\text{in}} = M$. If sweating is ignored, the rate of loss of energy by convection and radiation is approximately proportional to the amount by which the body temperature exceeds the ambient or surrounding temperature: $(dU/dt)_{\text{loss}} = K(T - T_a)$.

(a) What is the steady-state temperature as a function of M and T_a?
(b) Write a differential equation for T as a function of time. Suppose that M suddenly jumps by a fixed amount. What is the time constant?

Problem 11. When the body temperature is above 37 °C, sweating becomes important. The rate of energy loss is proportional to the amount of water evaporated. If all the perspiration evaporates, sweating loss can be approximated by $(dU/dt)_{\text{sweat}} = L(T - 37)$.

(a) Modify the differential equation of the previous problem to include $(dU/dt)_{\text{sweat}}$ as the input variable with T as the output variable. Combine it with this new equation to make a feedback loop. Determine the new equilibrium temperature and the time constant.

(b) Make numerical comparisons for the previous problem and this one when $M = 71$ kcal h^{-1}, $C = 70$ kcal °C^{-1}, $K = 25$ kcal h^{-1} °C^{-1}, $L = 750$ kcal h^{-1} °C^{-1}, $T_a = 38$ °C (high enough to ensure sweating).

Problem 12. A simplified model of the circulation is shown. Normally the arterial pressure is the same as that in the carotid sinus: $p_{\text{art}} = p_{\text{sinus}}$. In experiments on dogs whose vagus nerves were cut, the carotid arteries were isolated and perfused by a separate pump. This broke the feedback loop and allowed the curve on the accompanying graph to be obtained. The empirical equation shown (based on the work of Scher and Young (1963), summarized in Riggs (1970)) is (with pressures in torr)

$$p_{\text{art}} = 90 + \frac{120}{1 + \exp\left[(p_{\text{sinus}} - 165)/5\right]}.$$

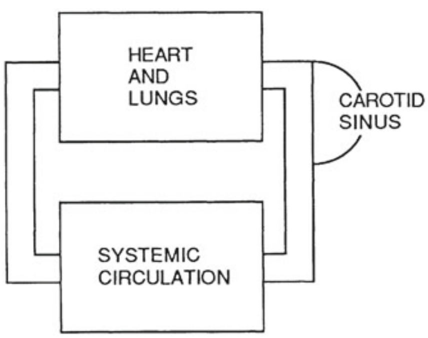

(a)

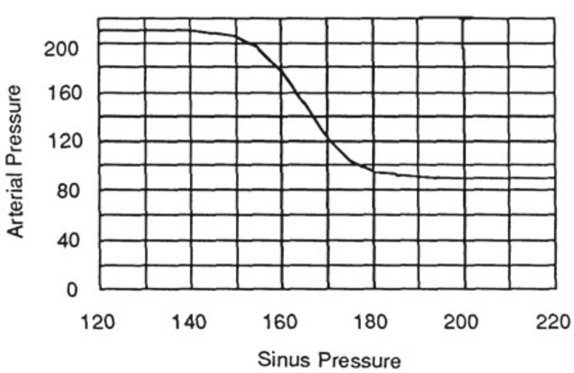

(b)

(a) Draw a block diagram of the complete feedback system. Label the blocks, show the functional relationship for each one, and indicate the proper cause-and-effect relationship.
(b) Find the operating point.
(c) Find the open-loop gain.

Problem 13. Consider the following special case of linear feedback: $\Delta x = G_1(\Delta p + \Delta y)$, $\Delta y = G_2 \Delta x$. Find the ratio $\Delta x/\Delta p$ when $G_1 \ll -1$, $G_2 < 1$.

Problem 14. Differentiate Eq. 10.4 and show that the expression for G_1 is the same as in Eq. 10.19.

Problem 15. For the thyroid problem, Problem 10.7, write a differential equation that can be solved to give C as a function of time. Suppose that at $t = 0$, R suddenly becomes 0. What is the differential equation then? Solve the equation; note that it is not linear.

Problem 16. The osmolarity of plasma (C, in mosmole) is regulated by the concentration of *antidiuretic hormone* (ADH, in pg ml^{-1}, also known as *vasopressin*). As antidiuretic hormone increases, the kidney reabsorbs more water and the plasma osmolarity decreases, $C = 700/ADH$. When osmoreceptors in the hypothalamus detect an increase of plasma osmolarity, they stimulate the pituitary gland to produce more antidiuretic hormone, $ADH = C - 280$ for C greater than 280, and zero otherwise.

(a) Draw a block diagram of the feedback loop, including accurate plots of the two relationships.
(b) Calculate the operating point and the open-loop gain (you may need to use four to six significant figures to determine the operating point accurately).
(c) Suppose the behavior of the kidney changed so now $C = 750/ADH$. First determine the new value of C if the regulation of ADH is not functioning (ADH is equal to that found in part (b), and then determine the value of C taking regulation of ADH by the hypothalamus into account.

Problem 17. The concentration of potassium ions in plasma K (in mM) is regulated by the concentration of the hormone aldosterone A (in ng per 100 ml). As aldosterone increases, the kidney excretes more potassium in the urine and the plasma concentration of potassium ions decreases: $K = 17.4/A$. When the extracellular potassium ion concentration rises, the adrenal gland produces more aldosterone: $A = (1/200)\exp(1.6K)$.

(a) Draw a block diagram of the feedback loop, including accurate plots of the two relationships.
(b) Calculate the operating point and the open-loop gain. (Note: you may have to find these numerically or graphically.)
(c) Suppose the behavior of the kidney changed so that $K = 20/A$. Determine the new value of K if the regulation of aldosterone is not functioning (A is equal to that found in part (b)), and then determine the value of K taking regulation of aldosterone into account.

Section 10.5

Problem 18. The following is a vastly oversimplified model of calcium regulation in dogs. Calcium is stored in body fluids and bones. Experiments show that the calcium concentration in the blood of a dog obeys approximately the equation (Riggs 1970, p. 491)

$$3.9\frac{dC}{dt} + 1.4C = 81.2 + \left(\frac{dQ}{dt}\right)_{\mathrm{iv}} + \left(\frac{dQ}{dt}\right)_r (t),$$

where C is the plasma concentration in mg l^{-1}, t is the time in h, $(dQ/dt)_{\mathrm{iv}}$ is the rate of intravenous infusion of calcium in mg h^{-1}, and $(dQ/dt)_r$ is the rate of reabsorption of calcium from bone into the blood in mg h^{-1}. (The numerical constants are consistent with these units.) The rate of reabsorption depends on the level of parathyroid hormone (PTH) concentration in the blood, which in turn depends on the calcium concentration. Instead of measuring the PTH concentration, experimenters found that $(dQ/dt)_r$ and C are related empirically by $(dQ/dt)_r = 188 - 1.34C$, where C is the independent variable.

(a) Draw a block diagram with variables $(dQ/dt)_r$ and C.
(b) Write equations to describe the steady state and find steady-state values of $(dQ/dt)_r$ and C when $(dQ/dt)_{\mathrm{iv}} = 0$.
(c) Find the open-loop gain.
(d) Find the time constant for the change of C when the parathyroid glands have been removed, in response to a step change in $(dQ/dt)_{\mathrm{iv}}$.
(e) Find the time constant for the change in C in response to a step change in calcium infusion when the parathyroid glands are intact, so that the feedback loop is closed.

Problem 19. This problem is a simplification by the authors suggested by the data of Chick et al. (1977) . Experimental data on diabetic rats show that the insulin level is 0 and the glucose level is 500. When an artificial pancreas is installed, a new operating point is reached for which $i = 40$ and $g = 100$.

(a) Make the simplest assumption possible: glucose level responds to insulin level according to $g = A + G_1 i$, while insulin responds to glucose as $i = G_2 g$. Find the open-loop gain.
(b) The same series of experiments showed that when the feedback loop is closed, the time constant for glucose to fall is 1.67 h. When the artificial pancreas is removed, the glucose level rises with a time constant of 10.67 h. Estimate the open-loop gain, assuming that the insulin level changes instantaneously.

Section 10.6

Problem 20. Multiply Eq. 10.28 by τ_2 and show that it reduces to Eq. 10.22 when $\tau_2 \ll \tau_1$.

Problem 21. For the two-stage feedback loop with equal time constants τ, show that oscillation results with a frequency $\omega = (|OLG|)^{1/2}/\tau$.

Problem 22. Consider two substances in the plasma with concentrations X and Y. (They might be glucose and insulin.) Assume that experiment has established the following facts.

(i) The steady-state values of each concentration are X_0 and Y_0. Departures from them are $x = X - X_0$ and $y = Y - Y_0$.
(ii) When $y = 0$, X is removed from the body at a rate proportional to x. This is true for both positive and negative values of x: $dx/dt = -(1/\tau_1)x$.
(iii) When $x = 0$, Y influences the rate at which X changes in an approximately linear fashion. An increase of Y above Y_0 ($y > 0$) increases the rate of disappearance of x.
(iv) When $x = 0$, y is cleared at a rate proportional to y: $dy/dt = -(1/\tau_2)y$.
(v) When $y = 0$ and x is nonzero, a positive value of x stimulates the production of Y, while a negative value of x inhibits the production of Y.

Assume that the rate of production is a linear function of x. Write down two linear differential equations to model these observations. That is, add a term to each of the equations given that describes observations (iii) and (v).

Problem 23. Combine the two equations obtained in the previous problem into a single differential equation in x. Show that it has the form

$$\frac{d^2x}{dt^2} + \left(\frac{1}{\tau_1} + \frac{1}{\tau_2}\right)\frac{dx}{dt} + \frac{1 - \mathrm{OLG}}{\tau_1\tau_2}x = 0.$$

Use the result of Problem 19 to obtain $1 - \mathrm{OLG}$ and suppose that $\tau_1 = 50$ min. For what value of τ_2 will critical damping occur? (If you find two values of τ_2, which seems more reasonable?) If τ_2 is greater than the value you select, will the system be overdamped or underdamped? (Do not take these results too seriously.)

Problem 24. This problem explores the behavior of a simple linear system from the point of view of the system's response to sinusoidal signals of various frequencies.

(a) The differential equation describing a system with time constant τ and gain G is

$$\frac{dx}{dt} = -\frac{1}{\tau}x + \frac{G}{\tau}y.$$

Show by substitution that if $y = Y \sin \omega t$, then $x = X \sin(\omega t + \phi)$, where $\tan\phi = \omega\tau$ and $X(\omega\tau \sin\phi + \cos\phi) = GY$.

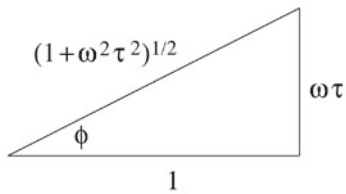

(b) Use the relation $\tan\phi = \omega\tau$ to establish the triangle shown, and use it to show that $X = GY/(1 + \omega^2\tau^2)^{1/2}$. These two relations give the response of the system in the frequency domain.

Problem 25. The following model for the attrition of troops in battle was developed by F. W. Lanchester and has been found to work reasonably well in several battles. The number of "friendly" troops is $F(t)$ and the number of "enemy" troops is $E(t)$. The rates of change are given by $dF/dt = -aE$, $dE/dt = -bF$, where a and b are the "effectiveness" of each side. The initial number of troops on each side is F_0 and E_0.
(a) What are the initial values of dF/dt and dE/dt?
(b) Obtain a differential equation for F.
(c) Find the most general solution to this differential equation and determine the coefficients from the initial conditions.
(d) Plot F and E for $a = b = 0.05$ and $E_0 = 2F_0$.

Problem 26. The equation $dF/dt = -aE$ of Problem 25 could also be thought of as describing a predator–prey situation if a represents the number of animals that the enemy eats per unit time. Ignoring latent periods such as gestation and infancy, what is the simplest way the equation could be modified to take account of reproduction and other ways of dying?

Section 10.8

Problem 27. Make a phase-space plot and discuss stability for $dy/dt = by$, $dy/dt = -by$, and $dy/dt = a - by$.

Problem 28. Make a drawing similar to Fig. 10.16 for the differential equation $dx/dt = x(c - x^2)$ for different values of c (positive and negative) and describe the stability of the fixed points as a function of c.

Problem 29. (a) Make drawings of the tip of the vector that defines θ' in Fig. 10.19 to show that when $b < 1$, θ' takes on all values, while for $b > 1$, θ' is restricted to values near 0 and 2π.
(b) Redraw Fig. 10.20a in the case that the angles are not reset to zero when they reach 2π.

Problem 30. Consider the undamped harmonic oscillator in the form $dx/dt = v$, $dv/dt = -\omega_0^2 x$.
(a) Make a phase-plane plot.
(b) Is the closed trajectory a limit cycle? Why or why not?
(c) Add a damping force proportional to $-v$ and redraw the phase-plane plot.

Problem 31. In Fig. 10.20, the phase behavior changes dramatically between $b = 0.95$ and $b = 1.05$. This change is most apparent for $\theta_s = \pi$, where $\theta' = 0$ for $b = 0.95$ and $\theta' = \pi$ for $b = 1.05$. What happens for $\theta_s = \pi$ and $b = 1$ exactly?

Problem 32. Reproduce qualitatively plots like Fig. 10.20 for $b = -0.95$ and $b = -1.05$. This corresponds to a hyperpolarizing stimulus.

Problem 33. Write a simple computer program to solve the two differential equations in Eq. 10.37 for $r(t)$ and $\theta(t)$. (See Sect. 6.14 for some guidance on how to solve differential equations numerically).
(a) Make plots of $x(t) = r(t)\cos(\theta(t))$ as a function of time for different stimuli.
(b) Reproduce a few points in the plots of Fig. 10.20 using your program. In particular, examine stimuli given at or near $\theta_s = \pi$ with b approximately equal to 1.
(c) Try varying the parameter a, and see how it affects the solution.

Problem 34. Use the program written in Problem 33 to examine entrainment. Stimulate the radial isochron clock periodically, with a frequency near but not exactly equal to the natural frequency of oscillation. Find examples where the clock is entrained to the stimulus (the oscillation has the same frequency as the stimulus).

Problem 35. A simple model for excitation of cardiac tissue is the FitzHugh–Nagumo model

$$\frac{dv}{dt} = \frac{1}{\varepsilon}\left(v - \frac{v^3}{3} - u\right)$$
$$\frac{du}{dt} = \varepsilon\,(v + \beta - \gamma u)\,,$$

where $\varepsilon = 0.2$, $\gamma = 0.5$ and $\beta = 0.8$.
(a) Make a plot in phase space (v versus u) of the *nullclines* (the curves obtained when $dv/dt = 0$ and $du/dt = 0$).
(b) Determine the steady-state solution (fixed point). You may have to do this numerically or graphically.
(c) Write a simple program to solve these equations on the computer. (See Sect. 6.14 for some guidance on how to solve differential equations numerically.) Plot $v(t)$ and $u(t)$ for the initial conditions $v(0) = -0.70$, $u(0) = -0.65$.

Problem 36. Edward Lorenz (1963) published a simple, three-variable (x, y, z) model of Rayleigh–Bénard convection:

$$\frac{dx}{dt} = \sigma(y - x)$$

$$\frac{dy}{dt} = x(\rho - z) - y$$
$$\frac{dz}{dt} = xy - \beta z$$

where $\sigma = 10$, $\rho = 28$, and $\beta = 8/3$.

(a) Which terms are nonlinear?
(b) Find the three equilibrium points for this system of equations.
(c) Write a simple program to solve these equations on the computer (see Sect. 6.14 for some guidance on how to solve differential equations numerically). Calculate and plot $x(t)$ as a function of t for different initial conditions. Consider two initial equations that are very similar, and compute how the solutions diverge as time goes by.
(d) Plot $z(t)$ vs. $x(t)$, with t acting as a parameter of the curve.

Problem 37. Consider the difference equation

$$x_{n+1} = \begin{cases} ax_n, & 0 < x_n < 0.5 \\ a(1 - x_n), & 0.5 < x < 1 \end{cases}$$

(a) Plot x_{n+1} vs. x_n for the case $a = 3/2$, producing a figure analogous to Fig. 10.23.
(b) Find the range of values of a for which the solution for large n does not diverge to infinity or decay to zero. You can do this using either arguments based on plots such as that in part (a) or numerical examples.
(c) Find the equilibrium value x^* as a function of a, using a method similar to that in Eq. 10.40.
(d) Determine if this value is stable or unstable, based on the magnitude of the slope of the x_{n+1} vs. x_n curve.
(e) For $a = 3/2$, calculate the first 20 values of x_n using 0.250 and 0.251 as initial conditions. Be sure to carry your calculations out to at least five significant figures. Do the results appear to be chaotic? Are the results sensitive to the initial conditions?
(f) For one of the data sets generated in part (e), plot x_{n+1} vs x_n for 20 values of n to create a plot analogous to Fig. 10.28. Explain how you could use this plot to distinguish chaotic data from a random list of numbers between zero and one.

Section 10.9

Problem 38. Show that for the logistic difference equation, the slope dx_{n+1}/dx_n at x^* is given by $2-a$, so that for $a > 3$ the slope has magnitude > 1.

Use a spreadsheet to plot x_n for different values of a and explore the period doubling.

Plot x_{j+1} vs. x_j, and show why we restricted a to values less than four.

For the logistic map with $a = 3.9$, evaluate x_j using the two initial conditions $x_1 = 0.2000$ and $x_1 = 0.2001$. Carry out the calculation for at least 20 iterations.

Problem 39. Cyclic variations in the population of a species are often studied with a predator–prey model such as the Lotka–Voltera equations (Chap. 2 Problem 38). It is also possible to have cyclic variations of a single species. This problem explores one such model and is based on Appendix B of Ginzburg and Colyvan (2004).

Let N_t represent the population at generation t. Let X represent the quality of the resources available to that species. R is the maximum growth rate, and $f(X)$ is a monotonically increasing function that asymptotically approaches unity for large X. The population in the next generation is

$$N_{t+1} = N_t R f(X_t).$$

If f is constant, we have exponential growth or decay, depending on whether Rf is greater or less than 1. We will model f by $f(X_t) = X_t/(k + X_t)$, where parameter k determines how rapidly f approaches its asymptotic value.

Now assume the total amount of food, S, does not change with time and that X depends on the per capita food supply S/N through a monotonically increasing function g:

$$X_{t+1} = X_t g(S/N_{t+1}).$$

A crucial assumption is that the current quality depends on both the present per capita food supply and the quality in the previous generation. When there is more food available to the mother, it increases the reproductive rate of the mother. Ginzburg and Colyvan call this the *maternal effect*.

Model functions f and g by

$$N_{t+1} = N_t R \frac{X_t}{k + X_t}$$
$$X_{t+1} = X_t M \frac{S/N_{t+1}}{p + S/N_{t+1}}.$$

(a) Show that with the change of variables $n = pN/S$ and $x = X/k$ the equations reduce to

$$n_{t+1} = n_t R \frac{x_t}{1 + x_t}$$
$$x_{t+1} = x_t M \frac{1}{1 + n_{t+1}}.$$

(b) Use a spread sheet to model the behavior for a range of values of R and M, starting with $R = 20$ and $M = 10$. Use initial conditions $n_0 = x_0 = 1$. If $M > 1$, explore what values of R lead to oscillations.
(c) Use the spread sheet to construct phase-plane plots of $\ln(n)$ vs $\ln(x)$.

Problem 40. Consider the two sets of data below, one produced by the logistic map and the other produced from a table of random numbers. Which is which?

Set 1	Set 2
0.9750	0.7464
0.0951	0.2349
0.3356	0.6017
0.8696	0.0213
0.4422	0.7935
0.9620	0.0336
0.1426	0.6476
0.4768	0.5630
0.9729	0.9116
0.1028	0.1748
0.3597	0.8706
0.8982	0.9058

Problem 41. The onset of ventricular fibrillation in the heart can be understood in part as a property of *cardiac restitution*. The action potential duration (APD) depends on the previous diastolic interval (DI): the time from the end of the last action potential until the start of the next one. The relationship between APD and DI is called the *restitution curve*. In cardiac muscle, a typical restitution curve has the form

$$APD_{i+1} = 300\left(1 - e^{-DI_i/100}\right)$$

where all times are given in ms. Suppose we apply to the heart a series of stimuli, with period (or "cycle length") CL.

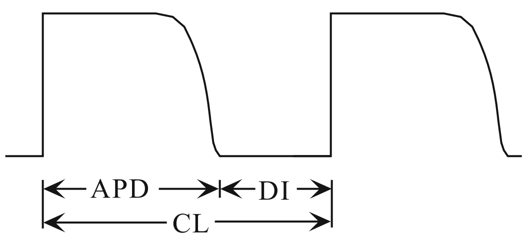

Since $APD + DI = CL$, we have $DI_{i+1} = CL - APD_{i+1}$.

(a) Suppose we stimulate with a long cycle length ($CL = 400$ ms). Using an initial value of $DI_1 = 200$, calculate APD_i and DI_i for ten iterations. What happens?

(b) Shorten the cycle length to $CL = 300$ ms. Using the same DI_1, calculate APD_i and DI_i for ten iterations. What happens now? (In the jargon of cardiac electrophysiology, this behavior is often called *alternans*).

(c) Shorten the cycle length further to $CL = 200$ ms. Using the same DI_1, calculate APD_i and DI_i for ten iterations. If DI_{i+1} is negative (corresponding to tissue so refractory that it fires no action potential), keep adding CL to it until it becomes positive before calculating the next APD. What happens now?

(d) Shorten the cycle length further to $CL = 100$ ms. Using the same DI_1, calculate APD_i and DI_i for twenty iterations. What happens now?

Your results in part (d) should be chaotic, resembling ventricular fibrillation. We must not overinterpret this simple model, however, because fibrillation consists of propagating wave fronts, whereas this simple model does not include spatial effects. For a more detailed account of a model similar to this one, see Hastings et al. (2000).

Problem 42. In Problem 41, the onset of alternans occurs when the slope of the restitution curve $APD_{i+1} = 300\left(1 - e^{-DI_i/100}\right)$ becomes greater than 1.

(a) Calculate the slope of the restitution curve $d(APD)/d(DI)$ analytically.

(b) Set the slope equal to 1 and solve for the resulting value of DI. Use the restitution curve to determine the corresponding values of APD and CL.

(c) Calculate APD_i and DI_i for twenty iterations for CL 10% above and 10 % below the value determined in part (b). What behaviors do you observe?

(d) Suppose you apply a drug to the heart that can change the restitution curve to $APD_{i+1} = 300\left(1 - be^{-DI_i/100}\right)$. Plot APD as a function of DI for $b = 0$, 0.5, and 1. What value of b ensures that the slope of the restitution curve is always less than 1? Garfinkel et al. (2000) have suggested that one way to prevent ventricular fibrillation is to use drugs that "flatten" the restitution curve.

Problem 43. Use the restitution curve from Problem 42 with $b = 1/3$ and $CL = 250$ to analyze the response of the system with initial diastolic intervals of 50, 60, 70, 80, and 90. You should find that the qualitative behavior depends on the initial condition. Which values of the initial diastolic interval give a 1 : 1 response? Which give 2 : 1? Determine the initial value of the DI to three significant figures for which the system makes a transition from one behavior to the other. When two qualitatively different behaviors can both occur, depending on the initial conditions, the system is *bistable*. To learn more about such behavior, see Yehia et al. (1999).

Problem 44. Elementary models of cellular excitable media (sometimes called *cellular automata*) provide valuable insight into the electrical behavior of the heart. Winfree (1987, pp. 106–107) describes one such model. A hexagonal array represents a sheet of cardiac tissue.

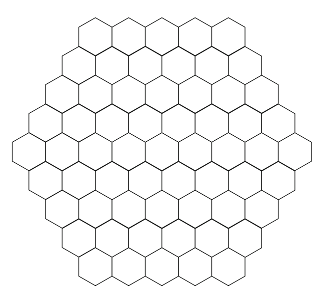

Each cell in the array can be in one of three states: excited (E), refractory (R), or quiescent (Q). A cell changes state by the following rules:

1. If in state E, then at the next time step it changes to state R,

2. If in state R, then at the next time step it changes to state Q,
3. If in state Q, then at the next time step it remains in state Q unless one of its six nearest neighbors is in state E, in which case it changes to state E.

(a) Start with the central cell in state E, and the rest of the cells in state Q. What happens in subsequent time steps? You should get an outwardly propagating wave front. Let the simulation run long enough to see what happens when the wave front hits the edge of the array. Does it "reflect" off the edge? Does the tissue ever go to the state of all Q?

(b) Start with the top five and bottom five cells in state E, and the rest in state Q. What happens when the two resulting wave fronts collide? Does the tissue ever go to the state of all Q?

(c) Start with the four black cells in state E, the three gray cells in state R, and the rest in state Q.

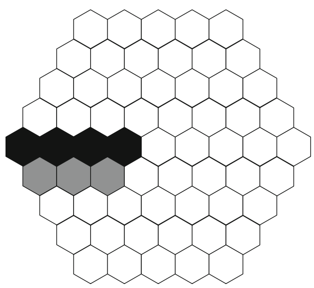

What happens? Does the tissue ever go to the state of all Q? This results in a spiral wave and may be responsible for some heart arrhythmias, such as ventricular tachycardia.

(d) In part (c), there is a special point called a *phase singularity* where cells in states E, R, and Q all meet at one point. Find the phase singularities in the results of part (c). How many are there? Do they move?

Problem 45. In the cellular excitable medium described in Problem 44, what happens if you apply an electrical stimulus? The stimulus is described by a fourth rule:

4. A stimulus changes the state to E, regardless of the previous state.

Assume the stimulus is applied only to the central cell. Start with the initial condition

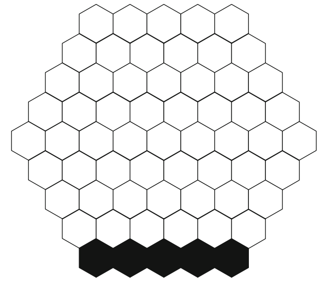

which will initiate a wave front propagating upward. At a later time, apply the stimulus and see what happens. If the initial condition is $t = 1$, then try applying the stimulus at $t = 4$, 5, or 6. Are there any situations in which you produce phase singularities? If so, how many? Is the timing of the stimulus important?

Section 10.10

Problem 46. By substitution show that $w(t) = w_0 e^{-\gamma t} \cos \omega t$ can be a solution of the delay-differential equation, Eq. 10.44 if $\gamma = (1/\tau)\, e^{\gamma t_d} \cos \omega t_d$, $\omega = (1/\tau)\, e^{\gamma t_d} \sin \omega t_d$. Introduce the dimensionless variables $\alpha = t_d/\tau$, $\xi = \omega t_d$, and $\eta = \gamma t_d$ and show that the result is the simultaneous equations $\xi = \alpha e^{\eta} \sin \xi$, $\eta = \alpha e^{\eta} \cos \xi$. From these obtain the equivalent equations $\eta = \xi \cot \xi$ and $\xi^2 = \alpha^2 e^{2\eta} - \eta^2$. Show how these can be solved graphically if α is known.

Section 10.12

Problem 47. Find an equation relating L, the total amount of light energy per second reaching the retina, I, the intensity of the light (W m^{-2}), and R, the radius of the pupil. Calculate the gain $G = \partial L/\partial R$ and the logarithmic gain $g = (1/L)(\partial L/\partial R)$. Consider the two cases shown in the figure.

(a) There is uniform illumination of the pupil.

(b) The rectangle of illumination partially overlaps the pupil so that the area within the pupil is $a(R - b)$.

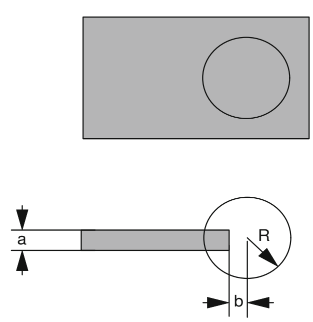

Problem 48. Suppose you measure the arrival time of an action potential wave front at four points (1–4) arranged in a diamond pattern each a distance b from a central point (open circle) located at (r_0, θ) relative to the origin. Use the steps below to calculate the wave front speed, direction, and curvature from these four measurements.

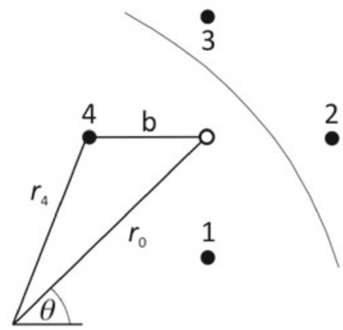

(a) Assume that the wave front is circular and propagates outward from the origin. Use the law of cosines to write r_1, r_2, r_3 and r_4 (the distance of each electrode from the origin) in terms of r_0, b and θ.
(b) Pull a factor r_0 outside the square root in each of your four expressions from part (a).
(c) Assume r_0 is much greater than b, and perform a Taylor expansion of each expression in terms of the small parameter $\xi = b/r_0$. Include terms that are constant, linear and quadratic in ξ.
(d) Write the arrival time at each of the four electrodes at $t_n = r_n/v$, where v is the wave speed.
(e) Let $\Delta t_{ij} = t_i - t_j$. Find expressions for Δt_{31} and Δt_{24} in terms of b, θ, and v. Solve these equations to determine v and θ in terms of Δt_{31}, Δt_{24}, and b.
(f) Find expressions for Δt_{14} and Δt_{23} in terms of b, θ, and v. Now (and this is the most difficult step), find an expression for the radius of curvature, r_0, in terms of b, Δt_{13}, Δt_{24}, Δt_{14}, and Δt_{23}.

Problem 49. Write a computer program to reproduce the numerical results in Fig. 10.35b and c. The calculation was originally performed by Glass and Mackey using the delay differential equation

$$\frac{dx}{dt} = \frac{\beta_0 x(t-\tau)}{1 + x^n(t-\tau)} - \gamma x(t)$$

where x is the white blood cell count (equal to P/θ in the figure), $\beta_0 = 0.2$, $\gamma = 0.1$, and $n = 10$. The initial condition for x is 0.1. Figure 10.35b uses $\tau = 6$, and Fig. 10.35c uses $\tau = 20$. (See Sect. 6.14 for some guidance on how to solve differential equations numerically.)

References

Abraham R, Shaw CD (1992) Dynamics: the geometry of behavior, 2nd ed. Addison-Wesley, Reading
Bartlett AA, Braun TJ (1983) Death in a hot tub: the physics of heat stroke. Am J Phys 51(2):127–132
Begon M, Mortimer M, Thompson DJ (1996) Population ecology: a unified study of animals and plants, 3rd ed. Blackwell Science, Cambridge
Bub G, Shrier A, Glass L (2002) Spiral wave generation in heterogeneous excitable media. Phys Rev Lett 88:058101
Chick WL et al. (1977) Artificial pancreas using living beta cells: effects on glucose homeostasis in diabetic rats. Science 197:780–781
Clayton RH, Bernus O, Cherry EM, Dierckx H, Fenton FH, Mirabella L, Panfilov AV, Sachse FB, Seemann G, Zhang H (2011) Models of cardiac tissue electrophysiology: progress, challenges and open questions. Prog Biophys Mol Biol 104:22–48
El-Samad H, Goff JP, Khammash M (2002) Calcium homeostasis and parturient hypocalcemia: an integral feedback perspective. J Theor Biol 214:17–29
Epstein AE, Ideker RE (1995) Ventricular fibrillation. In: Zipes DP, Jalife J (eds) Cardiac electrophysiology: from cell to bedside, 2nd ed. Saunders, Philadelphia, pp 927–933
Epstein IR, Kustin K, De Kepper P, Orban M (1983) Oscillating chemical reactions. Sci Am 248:112–123
Fox JJ, Bodenschatz E, Gilmour RF Jr (2002) Period-doubling instability and memory in cardiac tissue. Phys Rev Lett 89:138101
Garfinkel A, Spano ML, Ditto WL, Weiss JN (1992) Controlling cardiac chaos. Science 257:1230–1235
Garfinkel A, Kim Y-H, Voroshilovsky O, Qu Z, Kil JR, Lee M-H, Karagueuzian HS, Weiss JN, Chen P-S (2000) Preventing ventricular fibrillation by flattening cardiac restitution. Proc Natl Acad Sci U S A 97:6061–6066
Ginzburg L, Colyvan M (2004) Ecological orbits: how planets move and populations grow. Oxford University Press, Oxford
Glass L, Mackey MC (1988) From clocks to chaos. Princeton University Press, Princeton
Glass L, Nagai Y, Hall K, Talajic M, Nattel S (2002) Predicting the entrainment of reentrant cardiac waves using phase resetting curves. Phys Rev E Stat Nonlin Matter Phys 65:021908
Gray RA (2009) Rotors and spiral waves in the heart. In: Zipes DP, Jalife J (eds) Cardiac electrophysiology: from cell to bedside, 5th ed. Springer, New York, pp 349–360
Guevara MR, Glass L, Shrier A (1981) Phase-locking, period-doubling bifurcations, and irregular dynamics in periodically stimulated cardiac cells. Science 214:1350–1353
Guyton AC (1995) Textbook of medical physiology, 9th ed. Saunders–Elsevier, Philadelphia
Guyton AC, Crowell JW, Moore JW (1956) Basic oscillating mechanism of Cheyne–Stokes breathing. Am J Physiol 187:395–398
Hastings HM, Fenton FH, Evans SJ, Hotomaroglu O, Geetha J, Gittelson K, Nilson J, Garfinkel A (2000) Alternans and the onset of ventricular fibrillation. Phys Rev E 62:4043–4048
Hayes ND (1950) Roots of the transcendental equation associated with a certain difference-differential equation. J Lond Math Soc 25:226–232
Hilborn RC (2000) Chaos and nonlinear dynamics, 2nd ed. Oxford University Press, New York
Jalife J, Moe GK (1976) Effect of electrotonic potential on pacemaker activity of canine Purkinje fibers in relation to parasystole. Circ Res 39:801–808
Kaplan D, Glass L (1995) Understanding nonlinear dynamics. Springer, New York
Keener JP, Sneyd J (2008a) Mathematical physiology I: cellular physiology, 2nd ed. Springer, New York

Keener JP, Sneyd J (2008b) Mathematical physiology II: systems physiology, 2nd ed. Springer, New York

Khammash M, El-Samad H (2004) Systems biology: from physiology to gene regulation. IEEE Control Syst Mag 24:62–76

Khoo MCK (2000) Physiological control systems: analysis, simulation and estimation. IEEE, New York

Le Duc PR Messner WC Wikswo JP (2011) How do control-based approaches enter into biology? Annu Rev Biomed Eng 13:369–396

Lorenz EN (1963) Deterministic nonperiodic flow. J Atmos Sci 20:130–141

Luther S, Fenton FH, Kornreich BG, Squires A, Bittihn P, Hornung D, Zabel M, Flanders J, Gladuli A, Compoy L, Cherry EM, Luther G, Hasenfuss G, Krinsky VI, Pumir A, Gilmour RF, Bodenschatz E (2011) Low-energy control of electrical turbulence in the heart. Nature 475:235–239

Mackey MC, Glass L (1977) Oscillation and chaos in physiological control systems. Science 197:287–289

May RM (1976) Simple mathematical models with very complicated dynamics. Nature (London) 261:459–467

Mielczarek EV, Turner JS, Leiter D, Davis L (1983) Chemical clocks: experimental and theoretical models of nonlinear behavior. Am J Phys 51(1):32–42

Mines GR (1914) On circulating excitation on heart muscles and their possible relation to tachycardia and fibrillation. Trans R Soc Can 4:43–53

Murray JD (2007) Mathematical biology I: an introduction, 3rd ed. Springer, New York

Murray JD (2008) Mathematical biology II: spatial models and biomedical applications, 3rd ed. Springer, New York

Panfilov AV (2009) Theory of reentry. In: Zipes DP, Jalife J (eds) Cardiac electrophysiology: from cell to bedside, 5th ed. Saunders, Philadelphia, pp 329–338

Patton HD, Fuchs AF, Hille B, Scher AM, Steiner RF (eds) (1989) Textbook of physiology, 21st ed. Saunders, Philadelphia

Riggs DS (1970) Control theory and physiological feedback mechanisms. Williams and Wilkins, Baltimore

Scher AM, Young AC (1963) Servoanalysis of carotid sinus reflex effects on peripheral resistance. Circ Res 12:152–165

Stark L (1968) Neurological control systems: studies in bioengineering. Plenum, New York, pp 73–84

Stark LW (1984) The pupil as a paradigm for neurological control systems. IEEE Trans Biomed Eng 31:919–924

Stark L, Sherman PM (1957) A servoanalytic study of consensual pupil reflex to light. J Neurophysiol 20:17–26

Strogatz SH (1994) Nonlinear dynamics and chaos. Addison-Wesley, Reading

Strogatz SH (2003) Sync: the emerging science of spontaneous order. Hyperion, New York

Winfree AT (1987) When time breaks down. Princeton University Press, Princeton

Winfree AT (2001) The geometry of biological time, 2nd ed. Springer, New York

Witkowski FX, Kavanagh KM, Penkoske PA, Plonsey R (1993) In vivo estimation of cardiac transmembrane current. Circ Res 72(2):424–439

Witkowski FX, Plonsey R, Penkoske PA, Kavanagh KM (1994) Significance of inwardly directed transmembrane current in determination of local myocardial electrical activation during ventricular fibrillation. Circ Res 74(3):507–524

Witkowski FX, Kavanagh KM, Penkoske PA, Plonsey R, Spano ML, Ditto WL, Kaplan DT (1995) Evidence for determinism in ventricular fibrillation. Phys Rev Lett 75(6):1230–1233

Yehia AR, Jeandupeux D, Alonso F, Guevara MR (1999) Hysteresis and bistability in the direct transition from 1:1 to 2:1 rhythm in periodically driven single ventricular cells. Chaos 9:916–931